

NASA TECHNICAL NOTE



NASA TN D-2962

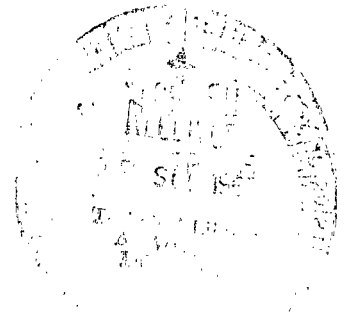
NASA TN D-2962

LOAN COPY: R  
AFWL (W  
KIRTLAND AF



NOISE STUDIES OF  
INLET-GUIDE-VANE—ROTOR  
INTERACTION OF A SINGLE-STAGE  
AXIAL-FLOW COMPRESSOR

*by John L. Crigler and W. Latham Copeland*  
*Langley Research Center*  
*Langley Station, Hampton, Va.*



TECH LIBRARY KAFB, NM



0079959

NOISE STUDIES OF INLET-GUIDE-VANE—ROTOR INTERACTION  
OF A SINGLE-STAGE AXIAL-FLOW COMPRESSOR

By John L. Crigler and W. Latham Copeland

Langley Research Center  
Langley Station, Hampton, Va.

NATIONAL AERONAUTICS AND SPACE ADMINISTRATION

For sale by the Clearinghouse for Federal Scientific and Technical Information  
Springfield, Virginia 22151 - Price \$2.00

NOISE STUDIES OF INLET-GUIDE-VANE—ROTOR INTERACTION  
OF A SINGLE-STAGE AXIAL-FLOW COMPRESSOR

By John L. Crigler and W. Latham Copeland  
Langley Research Center

SUMMARY

Some experimental results are presented of a noise study of a single-stage axial-flow compressor. The objective of the study was to investigate the effect of inlet-guide-vane—rotor interaction on the noise radiation patterns in the far field with a view toward alleviating the noise at its source. A variable-speed electric motor was used to drive the compressor rotor through a range of tip Mach numbers from 0.20 to 0.50. The test setup was arranged so that the number of inlet guide vanes could be varied and the vanes of each unit could be adjusted to give varying blade loading. Provisions for axial spacing of the rotor and guide vanes were made with the use of spacer rings.

The data are presented in the form of noise radiation patterns and frequency spectra. These data show how the radiation patterns are affected by the relative number of rotor blades and guide vanes. Calculations of radiation patterns were made for comparison with the experimental data, and good qualitative agreement was obtained. An increase in axial spacing of rotor and inlet guide vanes gave large reductions in noise levels when analyzed at the blade passage frequency, and furthermore the lobes of the noise radiation patterns were nearly eliminated. However, spacing had little effect on the overall noise radiation patterns.

INTRODUCTION

With the introduction of jet-powered commercial transports, the noise problem became a matter of great concern to the aircraft industry. In the early stages of the use of jet engines, the paramount problem appeared to be the noise due to the jet exhausts in take-off. Recently, however, it has become apparent that the noise during landing approach, particularly because of the presence of compressor noise components, is also of great concern. This concern has led to research aimed at compressor noise reduction.

Many studies have been made to obtain a better understanding of the compressor noise problem (e.g., refs. 1 to 6). These studies have dealt not only with the noise generation but also with the propagation of noise down the duct and its radiation from the face of the duct.

The present study relates to the effects of rotor—inlet-guide-vane interaction on the noise radiated to the far field with a view toward alleviating the noise at its source. In this study, use was made of a 14.75-in-diameter, single-stage, axial-flow compressor under controlled conditions in an anechoic test cell. A variable-speed electric motor was used to drive the compressor through a range of rotor tip Mach numbers from 0.20 to 0.50. The test setup was arranged so that the number of inlet guide vanes and the vane turning angle could be varied. Also, the axial spacing between the inlet guide vanes and rotor blades could be adjusted; this adjustment was accomplished with the use of a spacer ring. The data are presented in the form of noise radiation patterns and frequency spectra. The acoustic measurements are compared with normalized noise radiation patterns calculated by the method of reference 1 and are correlated with airflow measurements through the rotor.

### SYMBOLS

$a$	speed of sound
$B$	number of rotor blades
$c_{d,o}$	blade section profile drag coefficient
$c_l$	blade section lift coefficient
$k'_{m\mu}\sigma$	characteristic wave number
$k_{x\mu}$	wave number
$M_m$	circumferential tip Mach number for $m$ lobe pattern
$M_m^*$	cut-off Mach number
$M_t$	rotor tip Mach number, $N_t/a$
$m$	lobe number (difference between number of rotor blades and guide vanes)
$N$	rotor shaft speed, rpm
$N_t$	rotor tip speed, ft/sec
$n$	harmonic number
$r_o$	outer wall radius
$r_i$	inner wall radius

U	stream velocity
V	number of guide vanes
x	percent rotor tip radius
y	width of airfoil wake (see fig. 19)
$\mu$	radial mode index
$\xi_m$	cut-off ratio, $M_{tm}/M_{tm}^*$
$\sigma = \frac{r_i}{r_o}$	

## APPARATUS AND METHODS

### Description of Test Setup

A photograph of the test setup is shown as figure 1. The general physical arrangement of the compressor and drive motor is shown schematically in figure 2. The compressor consisted of a test rotor mounted in a suitable airflow duct which was annular in shape and which terminated in a large open space below floor level. The compressor was driven by a 52-hp variable-speed (rated 9000 rpm max.) electric motor at speeds up to 145 rps, which corresponded to a maximum tip speed of 560 ft/sec.

The test compressor consisted of a single-stage axial-flow rotor having 53 blades with root diameter of 10.72 in. and tip diameter of 14.75 in. The rotor blades were taken from one stage of a multiple-stage compressor of a jet engine. It was necessary to design the rotor wheel so that the blades could be set at the appropriate turning angle to obtain maximum efficiency when operated as a single-stage compressor. A photograph of the rotor wheel is shown as figure 3. The rotor blades had a NACA 65-series airfoil section with a constant chord of 0.70 in. Tests were made with and without guide vanes (constant chord of 0.70 in.) upstream of the rotor. Three guide-vane assemblies were used: 31 vanes, 53 vanes, and 62 vanes. The inlet guide vanes were from the stator associated with the rotor of the multiple-stage compressor; however, provisions were made to adjust the turning angle of the guide vanes so that the rotor blade loading could be varied. In most of the tests the turning angle of the guide vanes did not exceed 5°. Figure 4 is a photograph of the 53-guide-vane assembly.

Provisions were made for varying the guide-vane spacing (in guide-vane chords) ahead of the rotor from a minimum of 0.535 guide-vane chord (0.375 in.) to a maximum of 9.11 guide-vane chords (6.375 in.) by use of spacer rings. These rotor-inlet-guide-vane spacer rings were utilized with each of the three guide-vane assemblies.

The equipment was set up in a large anechoic chamber to minimize effects of wind, background noise, and so forth. The control station and recording equipment were located in the main data control room. The anechoic chamber and main data control room, located in the Langley noise research facility, are described in the appendix of reference 7. As indicated in figure 5, noise surveys were made in a horizontal plane containing the center line of the inlet duct and around a 12-ft-radius azimuth circle extending from near the 0° station (on the inlet axis) to the 90° station on this circle.

#### Noise Instrumentation

Seven commercially available condenser microphones were used at perpendicular incidence, and the output signals were recorded on a multichannel FM tape recorder. The overall response of the system from 20 cps to 10 000 cps, considered adequate for the blade passage frequency, was flat within  $\pm 2$  dB. The microphones were spaced at 15° intervals from 0° to 90°, as shown in figure 5; in addition, continuous sound recordings were made with the aid of a microphone that traversed this range of azimuth angles. For purpose of analysis, the tape recordings were played back into a graphic level recorder and one-third octave band analyzer.

#### Pressure Instrumentation

Six specially constructed pitot-static tubes were installed in the airflow upstream of the rotor and guide vanes to measure the flow properties. The pitot-static tubes were equally spaced across the duct. Commercially available pressure cells having a usable range of  $\pm 2$  psi were used to convert the output of these pitot-static tubes to electrical signals. The output signals of these pressure cells were recorded on a multichannel oscillograph located in the main data control room. Four additional pressure measuring devices (yawmeters) were located downstream of the rotor (fig. 2) to measure the pressure rise across the rotor.

#### Operating Procedures

The compressor was operated under various test conditions for the purpose of inlet noise surveys. For each test condition, noise data and compressor performance data were obtained for a range of rotor tip speeds. The runs were of the order of 2 to 3 minutes duration to permit satisfactory tape recording of the noise data and oscillograph recording of the pressure data. The measured radial velocity distribution through the compressor is shown for a range of rotor shaft speeds in figure 6 for the condition of no inlet guide vanes. An approximately uniform velocity profile exists across the duct at all rotor speeds. Figure 7 was plotted from the data of figure 6 to show the rate of airflow through the rotor as a function of the rotor shaft speed. The calculated weight flow, based on a knowledge of the rotor and its airfoil characteristics, has been included in the figure for comparison. The agreement between the measured and calculated values is excellent.

The tape recordings of the noise surveys have been analyzed in order to present the data in the form of radiation patterns and frequency spectra.

Input power to the compressor and compressor speed were recorded. Compressor speeds obtained for different test configurations were accurate within  $\pm 2$  rpm.

### THEORETICAL CONCEPTS

Experimental studies (for example, ref. 1) have dealt not only with the noise generated by the rotor or rotor-stator interactions but also with the propagation of the noise down the duct and its radiation from the face of the duct. Tyler and Sofrin (ref. 1) pointed out that the noise generated in the compressor is of the nature of rotating pressure patterns called "spinning modes." The spinning pressure modes may be generated by a compressor rotor or a rotor-stator combination. It is shown in reference 1 that a rotor-stator assembly produces pressure modes quite different from the spinning modes for the rotor alone. For the rotor alone, the pressure field consists of a single ( $nB$ )-lobe pattern which rotates with rotor angular velocity  $2\pi N$ ; consequently, an oscillating pressure is generated at a frequency of  $nBN$  cps. For the rotor-stator combination, as each rotor blade passes in the wake of a stator, an impulse of pressure is developed so that many patterns are formed, each of which has a number of lobes and a rotational speed that can be determined. (Although the impulse received at the rotor blade may be modified in amplitude and shape by the size and loading on the stator and by the distance between the stator vane and the rotor blade, it will have the same periodic recurrence.) Whether the pressure pattern propagates without a decrease in intensity to the end of the duct or decays along the duct depends on the speed with which it sweeps the duct walls, the crossover point or "cut-off" Mach number occurring when the propagating mode sweeps the duct walls at sonic speeds. The operating conditions for cut-off depend on the circumferential rotor tip Mach number, the lobe number (number of rotor blades for the no-stator condition or the difference in the number of rotor blades and stator vanes when a stator is used), and the hub-tip ratio. The cut-off Mach number for the rotor alone is not attained until the rotor tip speeds approach Mach 1.0; therefore, for the present tests on the rotor alone, the cut-off Mach number was not reached. For a rotor-stator combination, it is possible to form pressure patterns having rotational speeds above Mach 1.0 even though the rotor tip speed is much less than Mach 1.0. A method is outlined in reference 1 for computing the cut-off conditions for various rotor-stator configurations (or inlet-guide-vane-rotor configuration) and distinguishes the regions of propagation or decay along the duct. The circumferential tip Mach number is given by

$$M_m = \frac{BM_t}{m}$$

and the cut-off Mach number of the spinning  $m$  lobe pattern is

$$M_m^* = \frac{k_m' \mu \sigma}{m}$$

The wave number is then given by the relation

$$k_{x\mu} = \frac{m}{r_0} \sqrt{M_m^2 - (M_m^*)^2}$$

In this equation propagation exists when  $M_m > M_m^*$ , decay occurs when  $M_m < M_m^*$ , and at cut-off  $M_m = M_m^*$ . The cut-off ratio is

$$\xi_m = \frac{M_m}{M_m^*}$$

The cut-off ratios have been included in the data figures to readily indicate the conditions of decay or propagation. For convenience in calculating the cut-off Mach numbers for other configurations, figure 8 has been included, which is a plot of  $k'_{m\mu}\sigma$  as a function of  $m$  for two values of  $\sigma$  and for two values of the radial mode index  $\mu$ . Values of  $k'_{m\mu}\sigma$  may be calculated with the aid of reference 1 (fig. 11(a) and appendix II). For the range of  $\mu$  (fig. 8) the change in  $k'_{m\mu}\sigma$  for a given lobe number  $m$  is seen to be insignificant, particularly for a value of  $\mu = 1$ . The calculations in this report were made only for  $\mu = 1$ . Higher radial modes are of less significance because (1) the higher modes either do not propagate or begin to propagate at successively higher speeds than the  $\mu = 1$  mode and (2) the higher modes are further below the cut-off Mach number and decay more rapidly when the  $\mu = 1$  mode is decaying.

## RESULTS AND DISCUSSION

The results obtained in this study are presented in figures 9 to 21. Shown in figure 9 is the sound pressure level (SPL) of the one-third octave spectra at  $0^\circ$  azimuth for the rotor—53-guide-vane configuration. For this configuration the maximum noise peak is along the compressor axis. It can be seen that the maximum noise peak occurs at the fundamental blade passage frequency (6940 cps). The radiation patterns of the overall noise of the compressor for three rotor tip speed operating conditions for each inlet-guide-vane—rotor configuration and for the rotor alone are given in figure 10. As would be expected, in every case increasing the tip speed resulted in an increase in noise level. A further result for the rotor alone (fig. 10(a)) as well as for the rotor in combination with the 31 guide vanes (fig. 10(b)) and with the 62 guide vanes (fig. 10(c)) is that the radiation patterns tend to be nearly circular in shape; whereas, for the rotor in combination with the 53 guide vanes (fig. 10(d)) corresponding to the plane wave case ( $m = 0$ ) the peak noise level is on the  $0^\circ$  azimuth.

One-third octave band analyses were performed for the experimental data of the three rotor—inlet-guide-vane configurations of figure 10. The levels of the one-third octave analysis centered at the fundamental blade passage

frequency are compared with the calculated radiation patterns in figures 11 to 13. These calculated and measured data are normalized at the maximum values. The experimental radiation patterns for the rotor with the 53-guide-vane assembly ( $B = 53$ ,  $V = 53$ ,  $m = 0$ ) for two tip Mach numbers are compared with the calculated patterns in figure 11. Note that the peak of directivity patterns for both Mach numbers is on the  $0^\circ$  azimuth and both patterns are similarly lobed. However, the relative lobe peaks for the calculated patterns (particularly for  $M_t = 0.471$ ) are reduced markedly from those for the experimental pattern. The ratio of the spinning mode Mach number to the cut-off Mach number (i.e., the cut-off ratio  $\xi_m$ ) is given for each test condition and is seen to be much greater than 1.0. The measured and calculated radiation patterns for the rotor with the 62-guide-vane assembly ( $B = 53$ ,  $V = 62$ ,  $m = 9$ ) are shown in figure 12 for two rotor tip speeds. The calculations indicate generally the direction of maximum radiation and the number of lobes in the patterns. They do not, however, predict the detailed lobe structure of the pattern nor do they predict radiation in the direction of the axis of rotation, although the experimental results indicate a considerable pressure in this direction. Reference 1 (fig. 21(b)) indicated a similar trend. For the results in figures 11 and 12 over the range of  $M_t$  of the tests, the cut-off ratio is above 1.0 so that the noise pressure generated would be expected to propagate along the duct to the face of the duct, according to the findings of reference 1.

Measured and calculated radiation patterns for the rotor with the 31-guide-vane assembly ( $B = 53$ ,  $V = 31$ ,  $m = 22$ ) are presented in figure 13. The calculated radiation patterns indicate that the maximum noise level is near the  $90^\circ$  azimuth for both Mach numbers; whereas, the experimental pattern is lobed with several peaks having only small differences in the maximum values. The cut-off ratio for this configuration ( $B = 53$ ,  $V = 31$ ,  $m = 22$ ) for the range of  $M_t$  of the tests is shown in the figure to span the cut-off Mach number, results being given for  $\xi_m = 0.754$  and  $\xi_m = 1.086$ . For both values of  $M_t$  the peak of directivity for the calculated patterns is on the  $90^\circ$  azimuth. The measured data are not in agreement, even for  $\xi_m = 1.086$  where propagation of the generated noise pressure might be expected.

#### Effects of Spacers Between Inlet Guide Vanes and Rotor

The noise pressure patterns from the inlet-guide-vane—rotor combination is quite different from the pattern of the rotor alone. Experimental results in figure 14 showed that the sound pressure analyzed at blade passage frequency was markedly greater for the rotor operating in conjunction with a guide vane than when operating alone. These results, which are typical for the range of test rotor speeds, were obtained for a given rotor tip speed and a given pressure rise through the rotor for both the rotor with guide vanes and the rotor alone.

It appears that the differences noted are associated with the guide-vane—rotor interactions, which might be expected to vary with axial spacing between the guide vanes and rotor. Accordingly, tests were made with the three guide-vane assemblies previously discussed in this paper for three additional rotor— inlet-guide-vane spacings; the results are presented in figures 15 to 19. The

effect of rotor—inlet-guide-vane spacing on the generated noise for the rotor with the 62-guide-vane assembly at one tip Mach number (0.476) is shown in figure 15. Other guide-vane assemblies and rotational speeds showed similar trends. The rotor—guide-vane spacing was varied from 0.535 guide-vane chord (no spacer ring) to 9.11 chords. The noise level for the rotor without guide vanes is also shown in figure 15. The overall noise (fig. 15(a)) is not affected appreciably by rotor—guide-vane spacing over the range of the tests. Of greater significance, however, are the large reductions in the noise level when analyzed at the one-third octave band centered at the fundamental blade passage frequency (fig. 15(b)). The 6.25-guide-vane-chord spacing reduced the noise level of the rotor—guide-vane combination to approximately the level of the rotor alone at all angles except those above about the  $30^\circ$  azimuth angle. An increase in spacing to 9.11 chords resulted in a reduction in noise at the  $0^\circ$ ,  $15^\circ$ , and  $30^\circ$  azimuth angles to approximately the value obtained without guide vanes, but no further decrease in the noise level was indicated for the higher angles. For this configuration it appeared that only small noise reductions near the  $0^\circ$  azimuth are obtained with spacings larger than 6 guide-vane chords. For the tests of this figure, guide vanes were set at approximately the turning angle for zero lift and the rotor efficiencies were comparable for all configurations.

More detailed information relative to the reduction in noise obtained is given by radiation patterns analyzed at blade passage frequency, which are presented in figures 16 to 18. The effect of rotor—inlet-guide-vane spacing on the rotor with the 62 guide-vane assembly is shown in figure 16. In figure 16(a) the radiation patterns for the no spacer ring are compared with the radiation patterns for the 3.39-chord spacing and for the 6.25-chord spacing at a tip Mach number of 0.477. There is a general reduction in noise levels, and the individual lobes of the pattern except the one that peaks at approximately  $25^\circ$  azimuth are eliminated by the use of either spacer. As may be seen, there is a small decrease in noise level only in the  $0^\circ$  to  $45^\circ$  azimuth range when the spacing is increased from 3.39 to 6.25 chords. The results of increasing the spacing to 9.11 chords are presented in figure 16(b). It is readily observed that the lobe which peaks at about the  $25^\circ$  azimuth for the 6.25-chord spacing is eliminated with the 9.11-chord spacing, but no further decrease in the noise level was realized at other angles. Also shown in this figure is the noise radiation pattern for the rotor alone (no inlet guide vanes) at  $M_t = 0.477$ . Figure 17 compares the radiation patterns for the rotor—31-inlet-guide-vane configuration with no spacer ring, 3.39-chord spacing, and 6.25-chord spacing for a rotor tip Mach number of 0.498. A small reduction in noise levels was found with the 3.39-chord spacing; however, a large reduction in noise levels was obtained with the 6.25-chord spacing and the individual lobes of the pattern were eliminated. A further increase in spacing from 6.25 to 9.11 chords resulted in minor gains in noise reduction (not shown in the figure). In figure 18 are compared the radiation patterns for the rotor—53-inlet-guide-vane configuration ( $m = 0$ , the plane wave case) with no spacer ring, 3.39-chord spacing, and 6.25-chord spacing for a rotor tip Mach number of 0.471. The peak of directivity pattern, as previously discussed for this case, is on the  $0^\circ$  azimuth, and this peak has been appreciably reduced with the use of spacers, the greatest reduction in noise levels being realized with the 6.25-chord spacing. The changes in noise levels away from the vicinity of  $0^\circ$  azimuth were generally small. It can be seen from the results of the assemblies

tested (62, 31, and 53 inlet guide vanes) that the effect of spacing on the one-third octave band noise radiation patterns is appreciable.

These results indicate a need for further study of the effect of axial spacing of the inlet guide vanes and the first-stage rotor of a multiple-stage compressor and, also, the effect of stator vanes downstream of the rotor.

The effect of spacing on the noise spectra is illustrated in figure 9. Spectra are shown for the 0.53-chord spacing (no spacer ring) and the 6.25-chord spacing. Three main features of these spectra can be noted. The maximum noise peak occurs at the higher frequencies in the vicinity of 7000 cps. This noise peak is in the frequency range of the fundamental blade passage frequency. Also, at the frequencies in the vicinity of 500 to 3000 cps, the amplitude of the noise is considerably lower and there is very little difference in the spectral content in this frequency range for the two chord spacings. Finally, the high noise peak exhibited with the 0.535-chord spacing has been greatly reduced with the 6.25-chord spacing. In fact, the noise level was reduced by 10 to 14 dB in the 6500-to-7500-cps frequency range with the 6.25-chord spacing.

Because large differences in noise pressure were realized with increased spacing, an attempt has been made to see how these differences correlated with the flow details in the wake of the guide vanes. Reference 8 gives a method by which the important wake parameters in terms of the distance behind the airfoil trailing edge and of the profile drag coefficient  $c_{d,o}$  can be determined. Experimental data in reference 8 (fig. 33) indicate that for a given airfoil the wake is displaced downward with an increase in  $c_l$  (increase in angle of attack) and that the change in wake velocity profile with  $c_l$  is relatively small up to the angle of stall, the main wake parameters being a function of the profile drag and the distance behind the airfoil. In summary, then, it does not appear that changes in the loading on the guide vanes up to near stall should appreciably affect the defect in velocity in the wake.

The viscous wakes of airfoils in cascade as calculated by the method of reference 8 are shown in figure 19. The calculations were made for a value of  $c_{d,o}$  of 0.01, which is considered representative for the airfoils used for guide vanes. The wake width and the reduction in velocity across the wake (velocity defect) in terms of the stream velocity are shown as a function of the distance behind the airfoil, expressed in guide-vane chords. The figure shows that at 0.535 chord behind the trailing edge of the airfoil the wake width was only 0.12 chord and that the velocity on the center line of the wake was only 85.5 percent of the stream velocity. The velocity defects attenuate downstream rapidly and at a distance of 6.25 chords behind the trailing edge of the airfoil the minimum velocity in the center of the wake is only 1.9 percent below stream velocity, and the wake width is now increased to 0.364 chord. However, the velocity defects in the wake cause instantaneous increases in the angles of attack of the rotor blade which, in turn, result in instantaneous increases in blade loading and in a small increase in the average loading. The results of the present investigation suggest that the noise increase associated with the rotor-inlet-guide-vane interaction is due to the presence of the instantaneous increases in blade loading rather than the small average increase in blade

loading due to the presence of the guide-vane wakes. It would be expected, then, that an increase in rotor-inlet-guide-vane spacing would have a favorable effect on the interaction noise regardless of the loading on the guide vanes.

### Effect of Stage Loading on Noise Generated

The results for all previous tests were obtained for near-zero loading on the guide vanes in order to get comparable operating conditions without guide vanes. The measured radiation patterns analyzed at the blade passage frequency for the rotor with the 62-inlet-guide-vane assembly for two angle settings of the guide vanes and at the same rotor tip Mach number are presented in figure 20. The method of calculation of reference 1 does not account for a change in rotor loading. The guide vanes were set at  $-5^\circ$ , approximately the zero turning angle, in one case and then increased by  $15^\circ$  to  $+10^\circ$ . This increase in guide-vane angle would, of course, increase the steady-state loading on the rotor blades, but the change in oscillating air forces for the two angles due to the velocity defect in the wake would be small. The horsepower absorbed by the rotor is seen in the figure to increase approximately 20 percent for the higher guide-vane angle ( $10^\circ$ ) for constant rotor speed. The experimental data in the figure are made for relative noise levels, as was done in figure 14, so that direct comparisons can be made with the calculated pattern. The maximum noise level for both sets of experimental data and for the calculated curve occurred near the  $30^\circ$  azimuth angle with the peak noise level for the higher rotor loading occurring at the slightly higher azimuth angle. As was noted in figure 14, the experimental data show a lobe near the axis (about the  $5^\circ$  azimuth angle) which was not present in the calculated data. The peak noise level of the lobe of this azimuth angle was about 7 dB higher for the higher rotor loading than for the lower loading. On the other hand, the peak noise level of the lobe near the  $50^\circ$  azimuth angle was about 5 dB higher for the lower rotor loading than for the higher loading. These results indicate that the noise radiation pattern of the fundamental blade passage frequency is a function of the rotor loading, a variable not considered in the calculated radiation patterns.

The radiation patterns of the overall noise for the two loading conditions of figure 20 are given in figure 21. The changes in the overall noise radiation patterns with this range of loading conditions are small.

### CONCLUSIONS

Noise studies conducted with a single-stage compressor in an anechoic chamber over a range of rotor tip speeds for a 53-blade rotor with various inlet-guide-vane configurations indicate the following conclusions:

1. The overall noise radiation patterns were nearly circular in shape (not highly directional), and the radiation patterns at the blade passage frequency exhibited lobes. The number of lobes was dependent upon the inlet-guide-vane-rotor configuration, that is, the number of vanes and the rotational speed.

2. The calculations permit the determination on a qualitative basis of noise radiation patterns which are in good agreement with experimental patterns in the range for spinning modes above cut-off Mach number, that is, in the range for propagation; however, in the range below cut-off, in the region of decay, the experimental noise radiation patterns have little similarity with calculated patterns.

3. An increase in axial spacing of rotor and guide vanes gave large reductions in noise levels when analyzed at the blade passage frequency and, furthermore, the lobes of the noise radiation patterns were nearly eliminated. However, spacing had little effect on the overall noise radiation patterns.

4. A change in guide-vane loading with a resulting change in rotor blade loading has an effect on the noise radiation patterns when analyzed at the blade passage frequency but has little effect on the overall noise radiation patterns at constant rotor tip speed.

Langley Research Center,  
National Aeronautics and Space Administration,  
Langley Station, Hampton, Va., May 24, 1965.

#### REFERENCES

1. Tyler, J. M.; and Sofrin, T. G.: Axial Flow Compressor Noise Studies. [Preprint] 345D, Soc. Automotive Engrs., 1961.
2. Greatrex, F. B.: By-Pass Engine Noise. Preprint No. 162C, Soc. Automotive Engrs., Apr. 1960.
3. Griffiths, J. W. R.: The Spectrum of Compressor Noise of a Jet Engine. J. Sound Vib., vol. 1, no. 2, Apr. 1964, pp. 127-140.
4. Morfey, C. L.: Rotating Pressure Patterns in Ducts: Their Generation and Transmission. J. Sound Vib., vol. 1, no. 1, Jan. 1964, pp. 60-87.
5. Bragg, S. L.; and Bridge, R.: Noise From Turbojet Compressors. J. Roy. Aeron. Soc., vol. 68, no. 637, Jan. 1964, pp. 1-10.
6. Copeland W. Latham: Inlet Noise Studies for an Axial-Flow Single-Stage Compressor. NASA TN D-2615, 1965.
7. Kantarges, George T.; and Cawthorn, Jimmy M.: Effects of Temperature on Noise of Bypass Jets as Measured in the Langley Noise Research Facility. NASA TN D-2378, 1964.
8. Silverstein, Abe; Katzoff, S.; and Bullivant, W. Kenneth: Downwash and Wake Behind Plain and Flapped Airfoils. NACA Rept. 651, 1939.

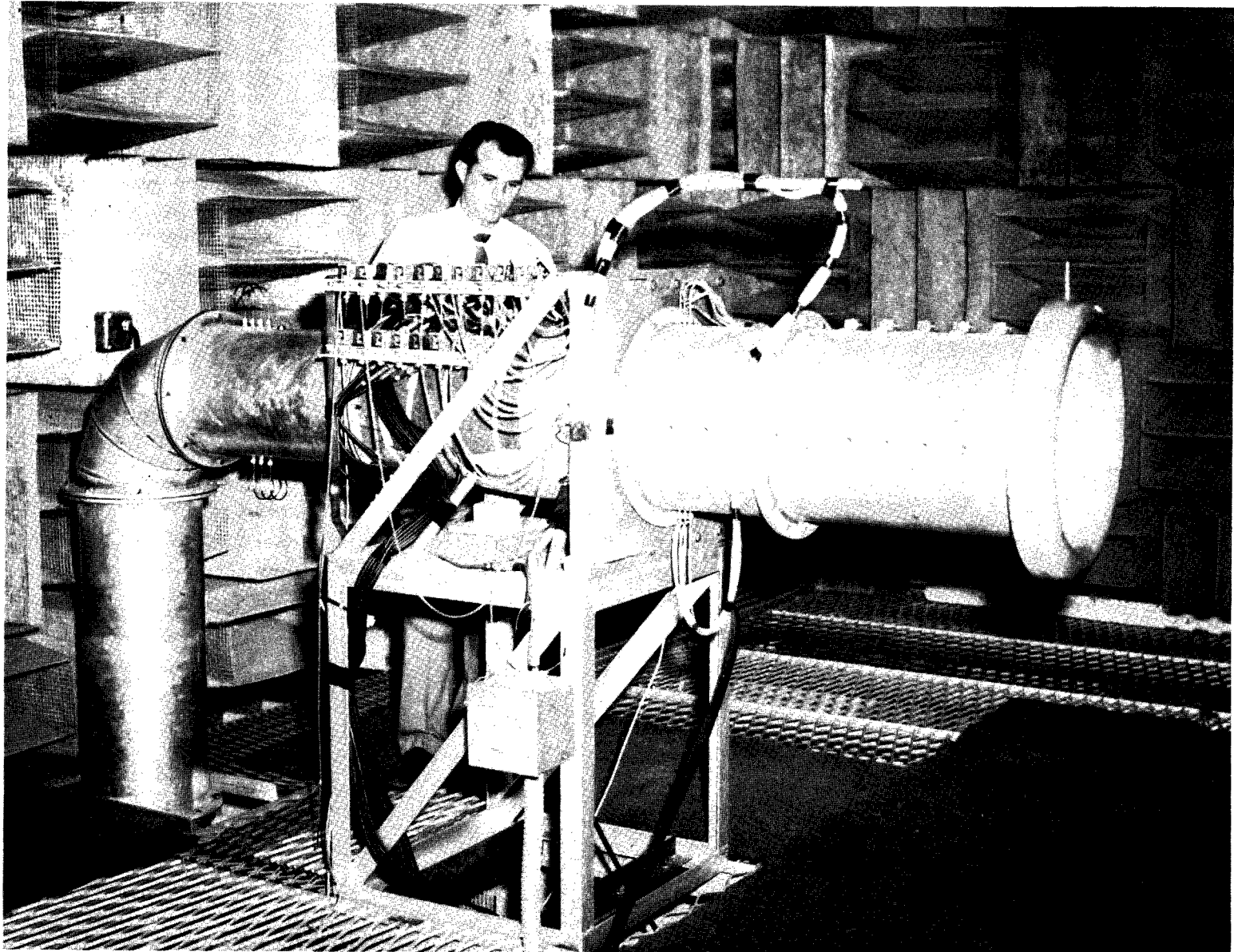


Figure 1.- Test compressor mounted in anechoic cell.

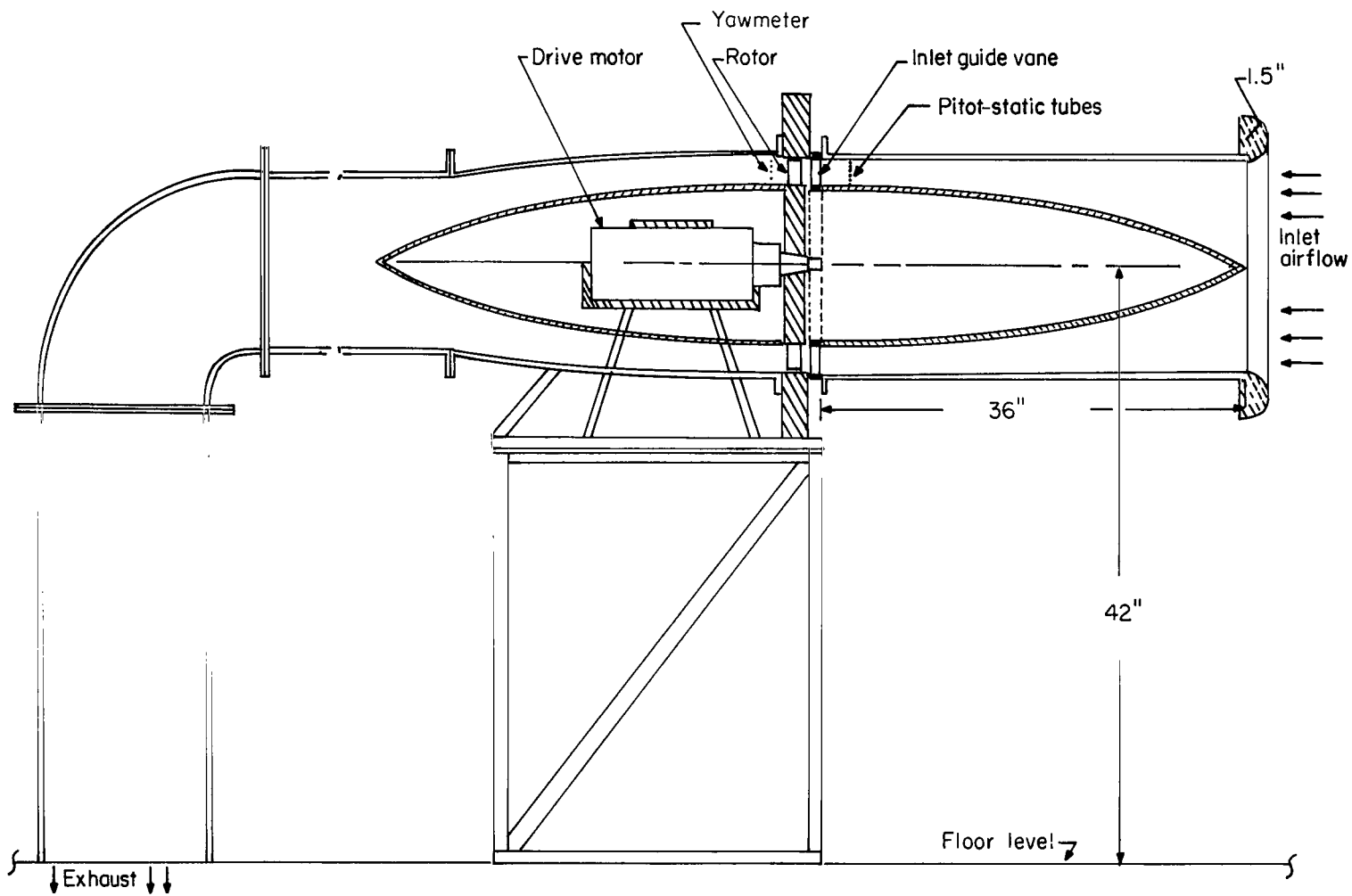


Figure 2.- Schematic of test compressor.



Figure 3.- Rotor wheel with blades.

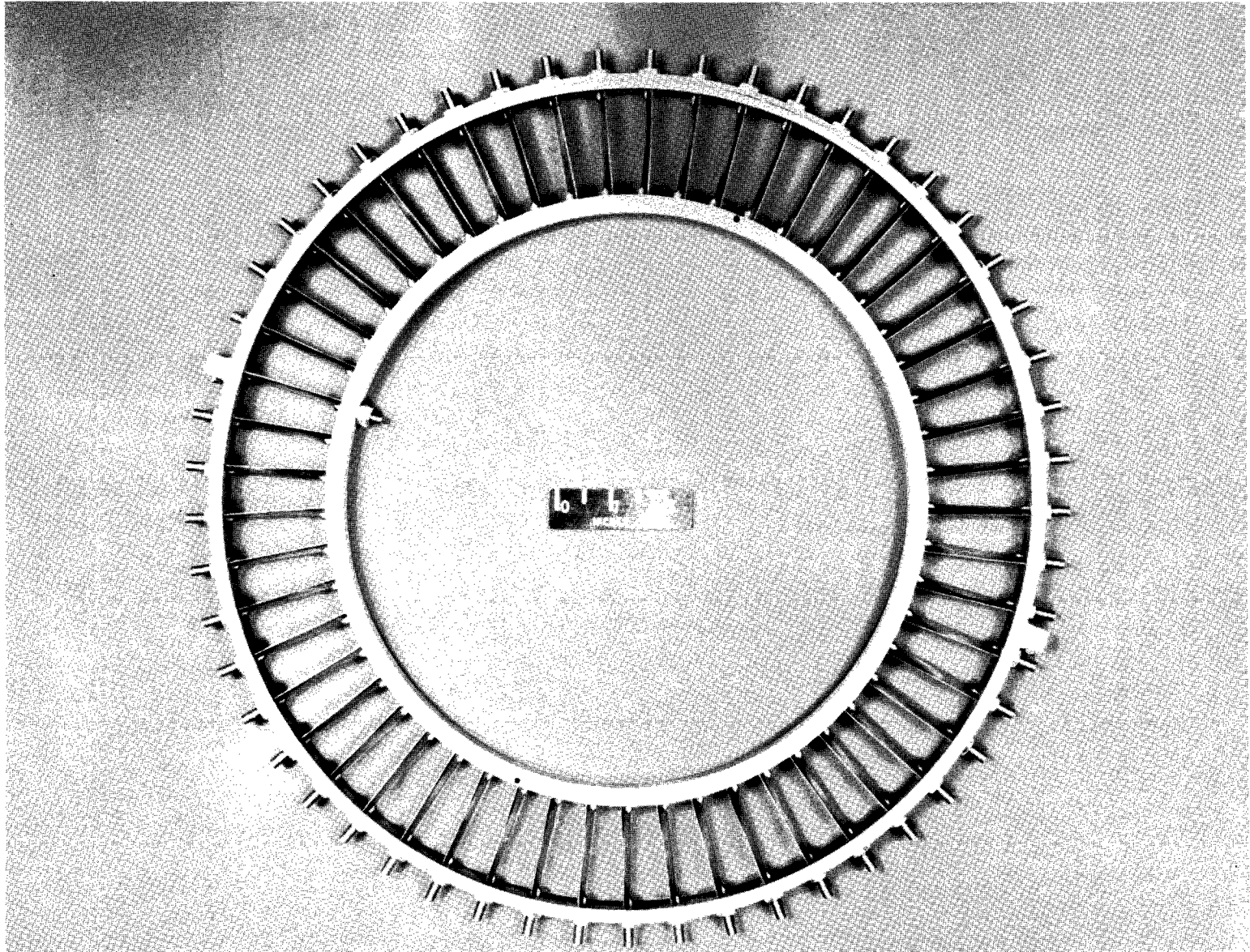


Figure 4.- Inlet-guide-vane assembly with 53 vanes.

L-63-3783

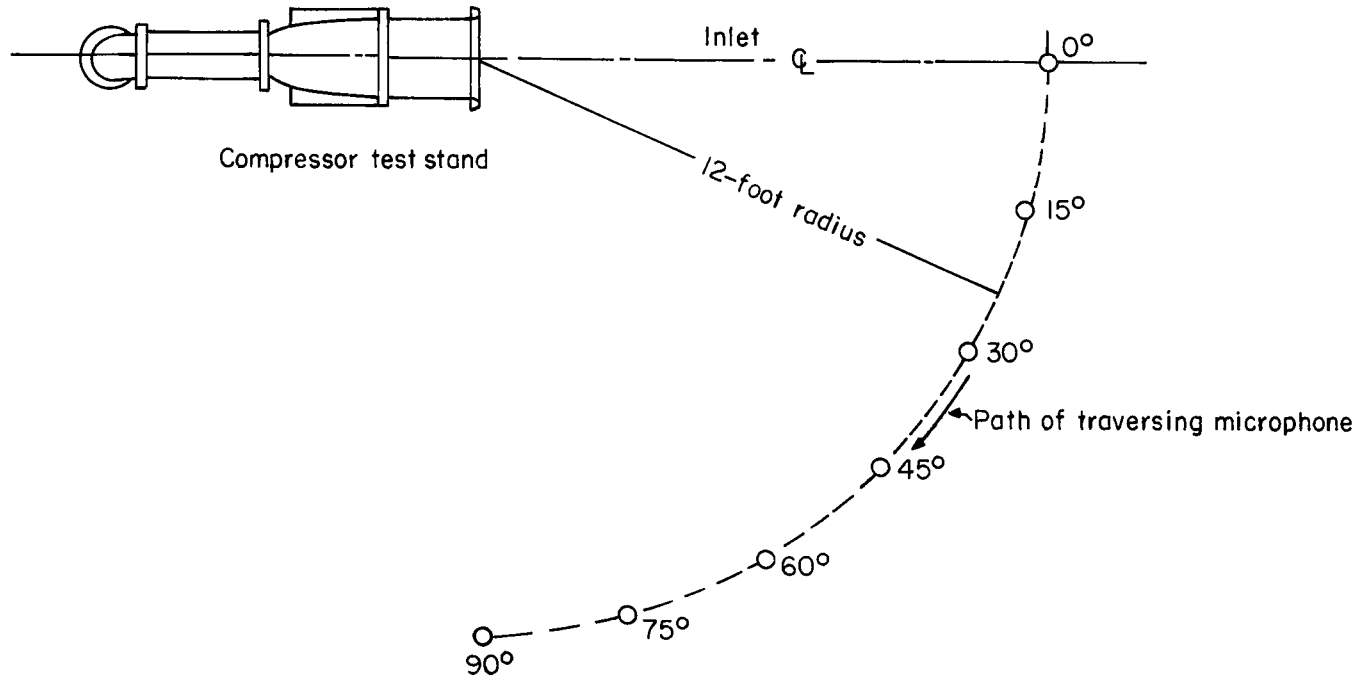


Figure 5.- Plan view showing location of microphones.

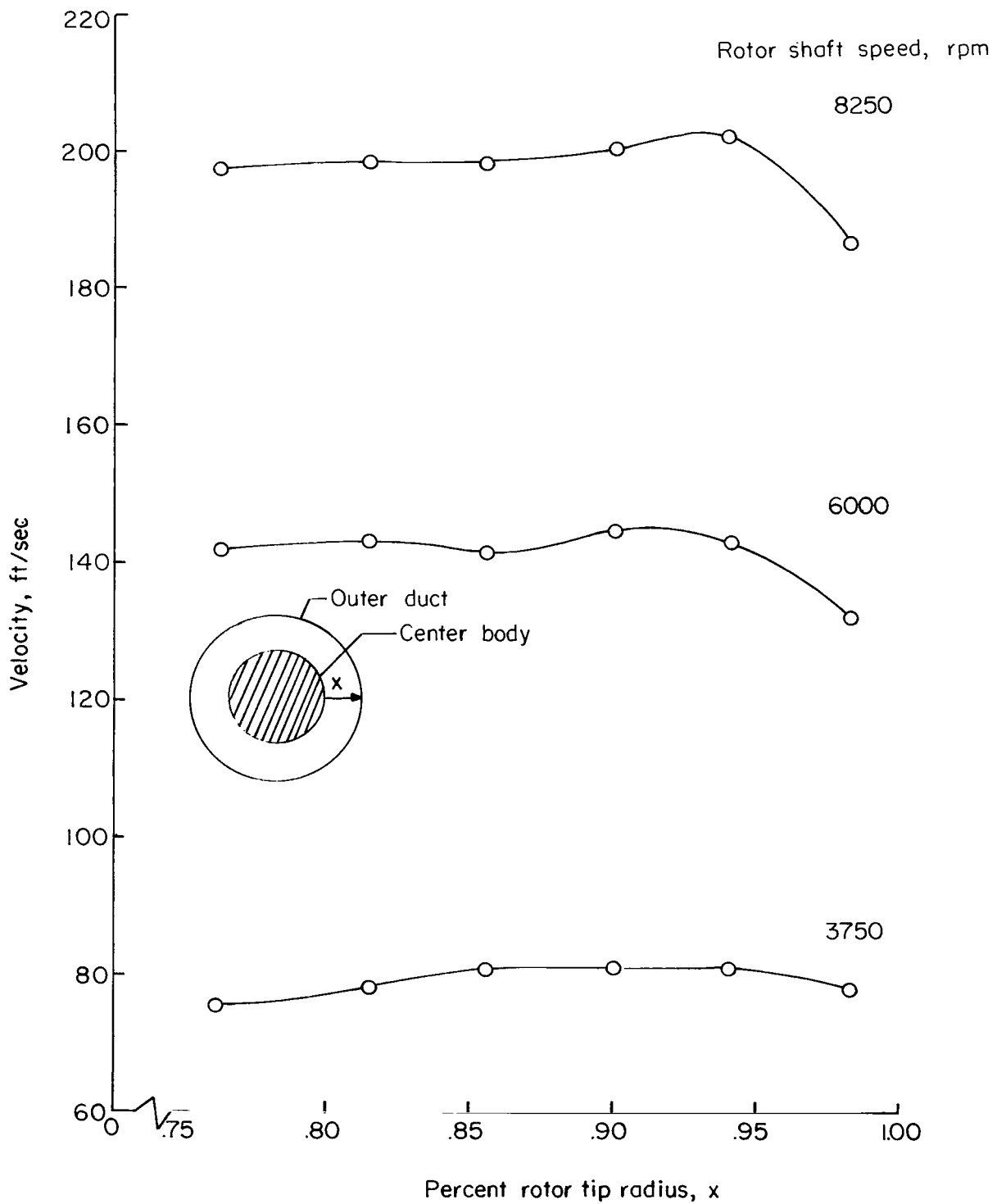


Figure 6.- Measured inlet velocity distribution in inlet duct. (No inlet guide vanes.)

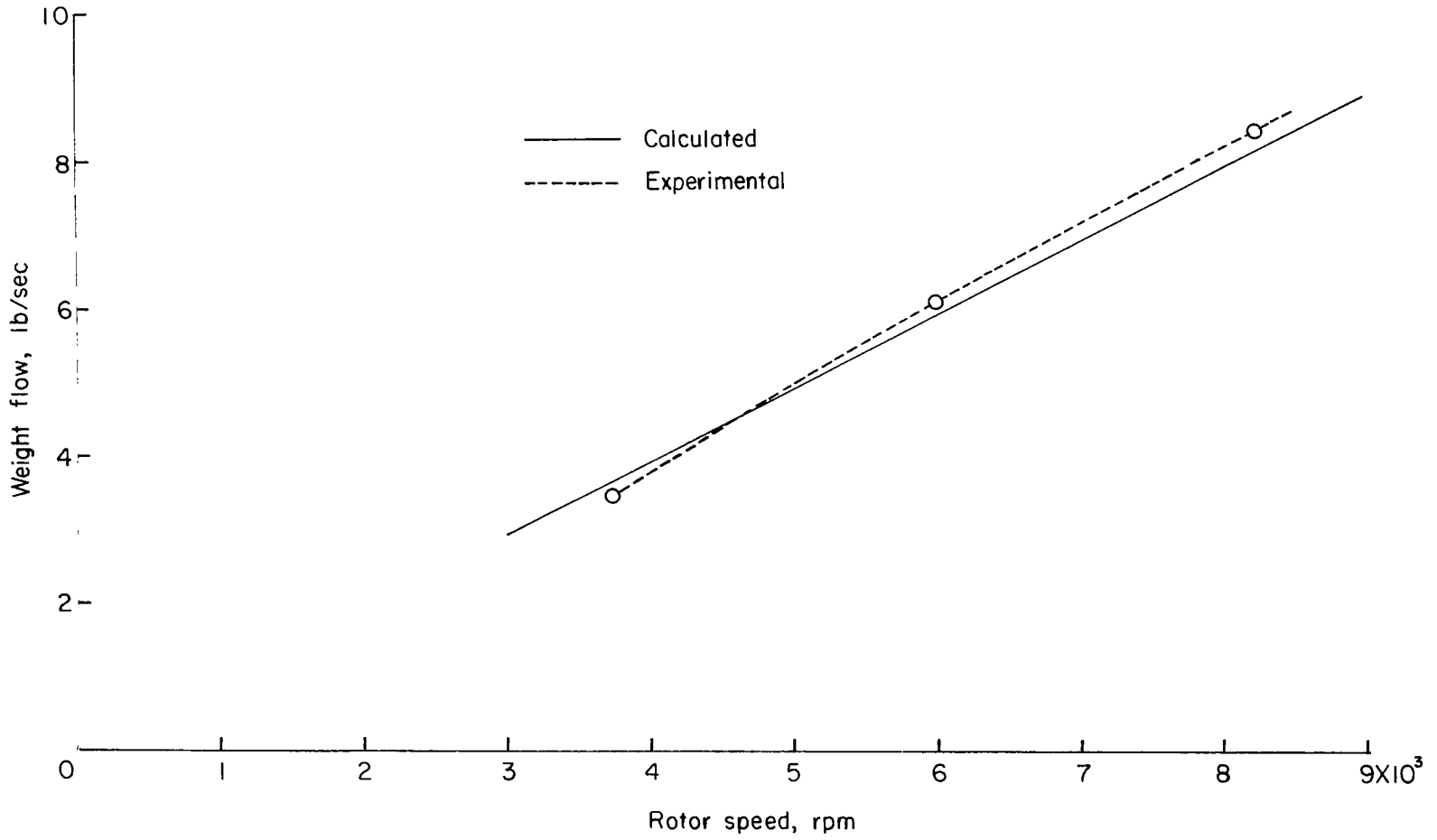


Figure 7.- Variation of mass flow with rotor speed for rotor alone.

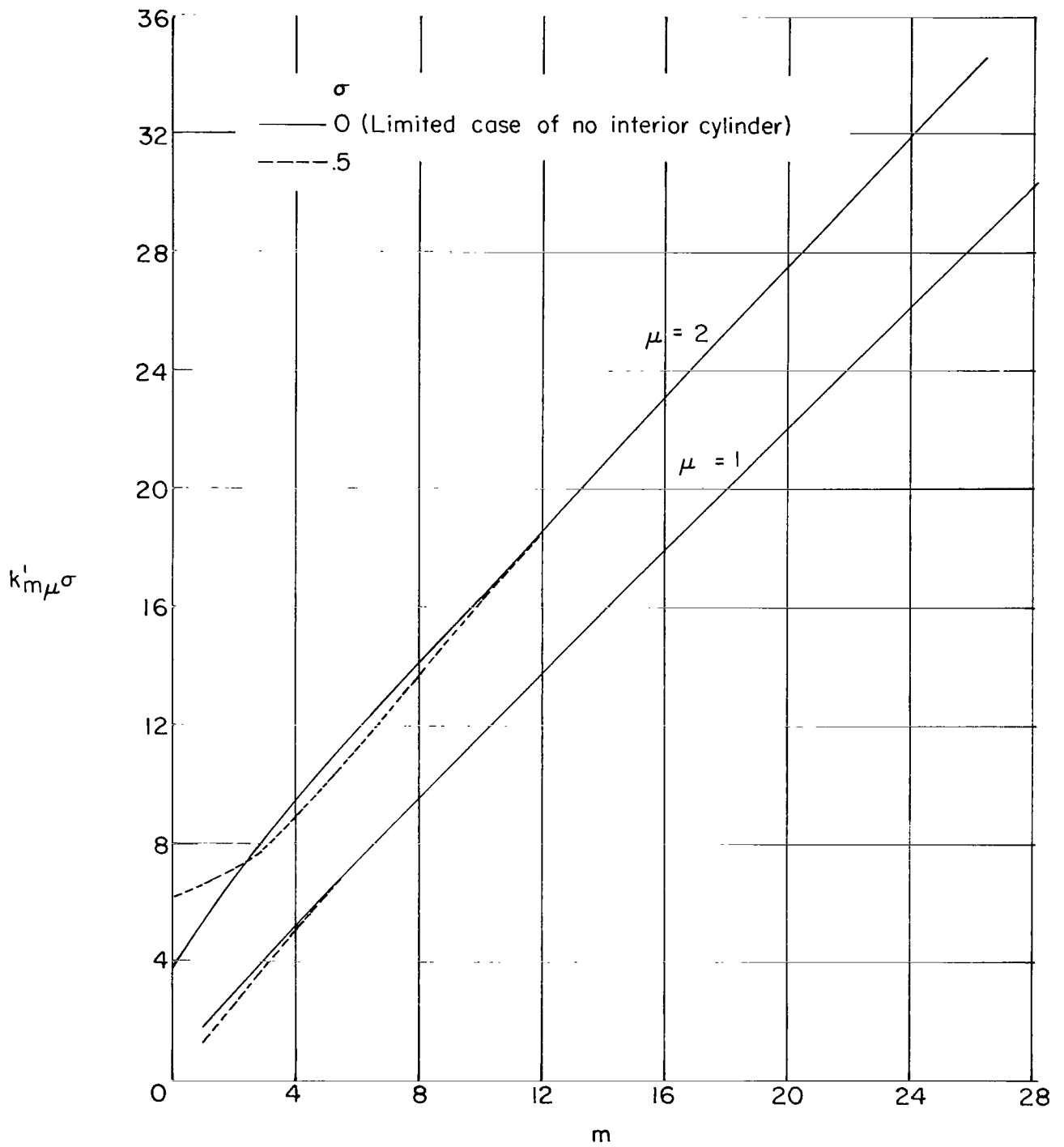


Figure 8.- Characteristic wave number as a function of lobe number.

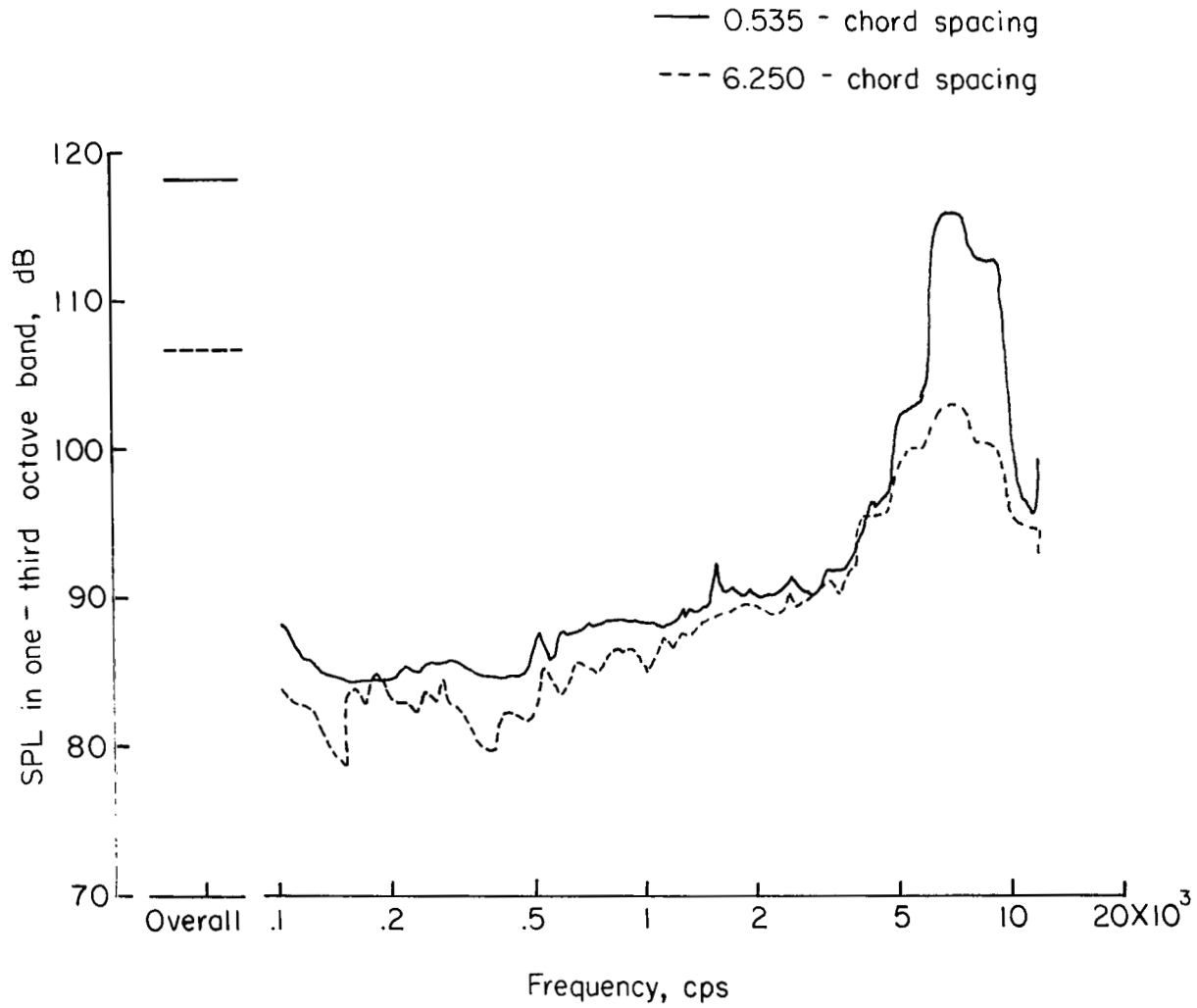
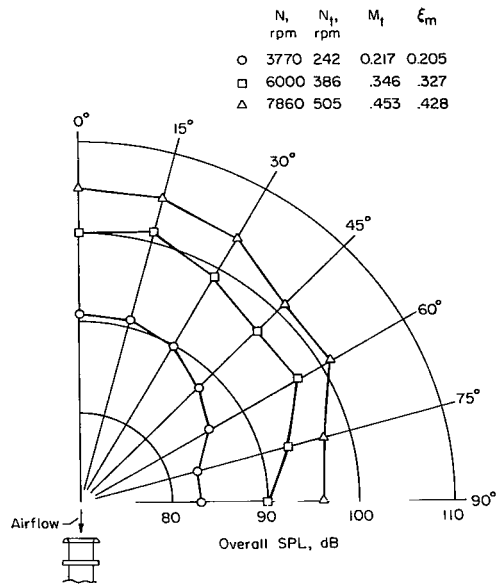
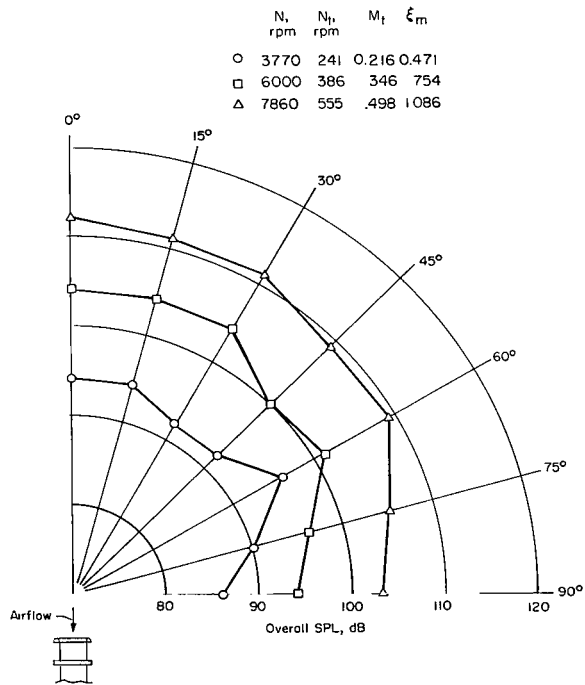


Figure 9.- One-third octave band spectra at  $0^\circ$  azimuth for the rotor-53-guide-vane configuration with two rotor-guide-vane spacings.  $M_t = 0.453$ .

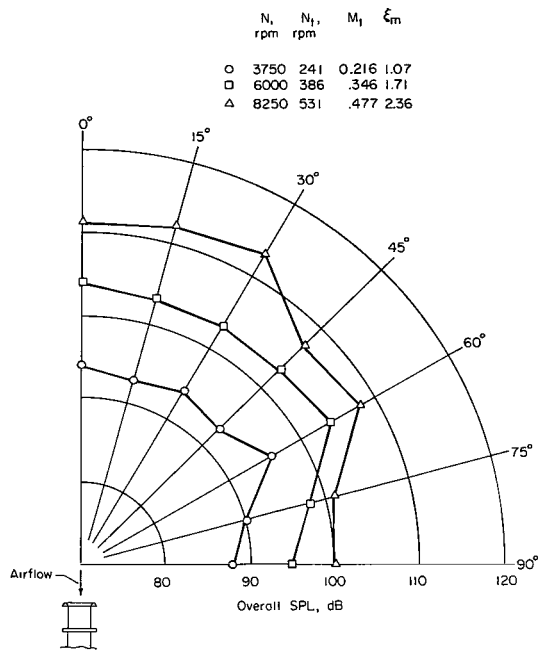


(a) Rotor alone (no guide vanes).

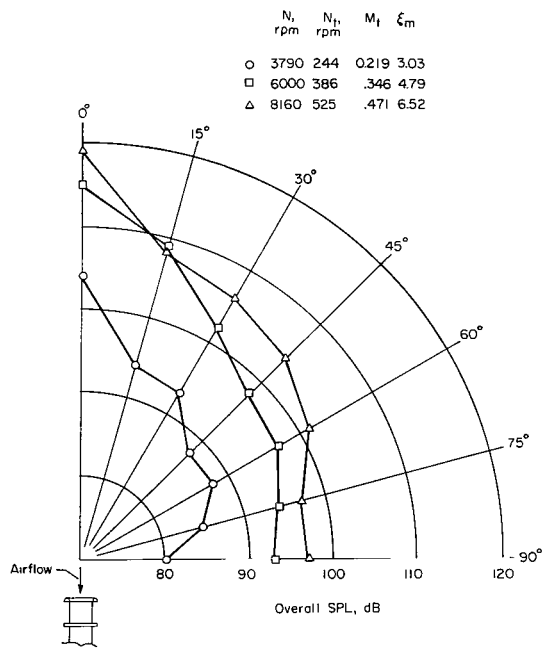


(b) Rotor with 31 guide vanes.

Figure 10.- Overall noise radiation patterns measured on a 12-foot radius for different rotor speeds and rotor-guide-vane configurations.

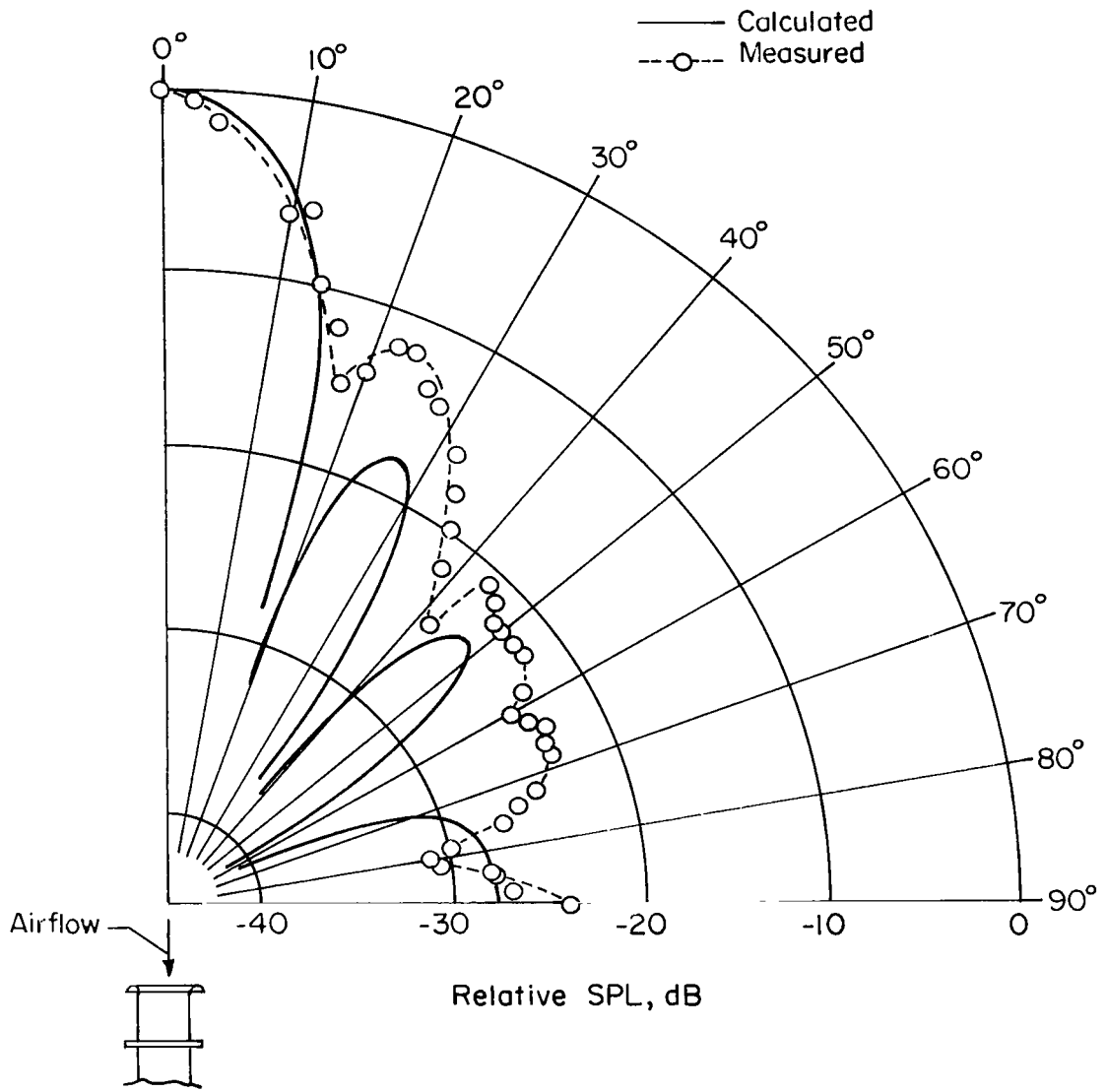


(c) Rotor with 62 guide vanes.



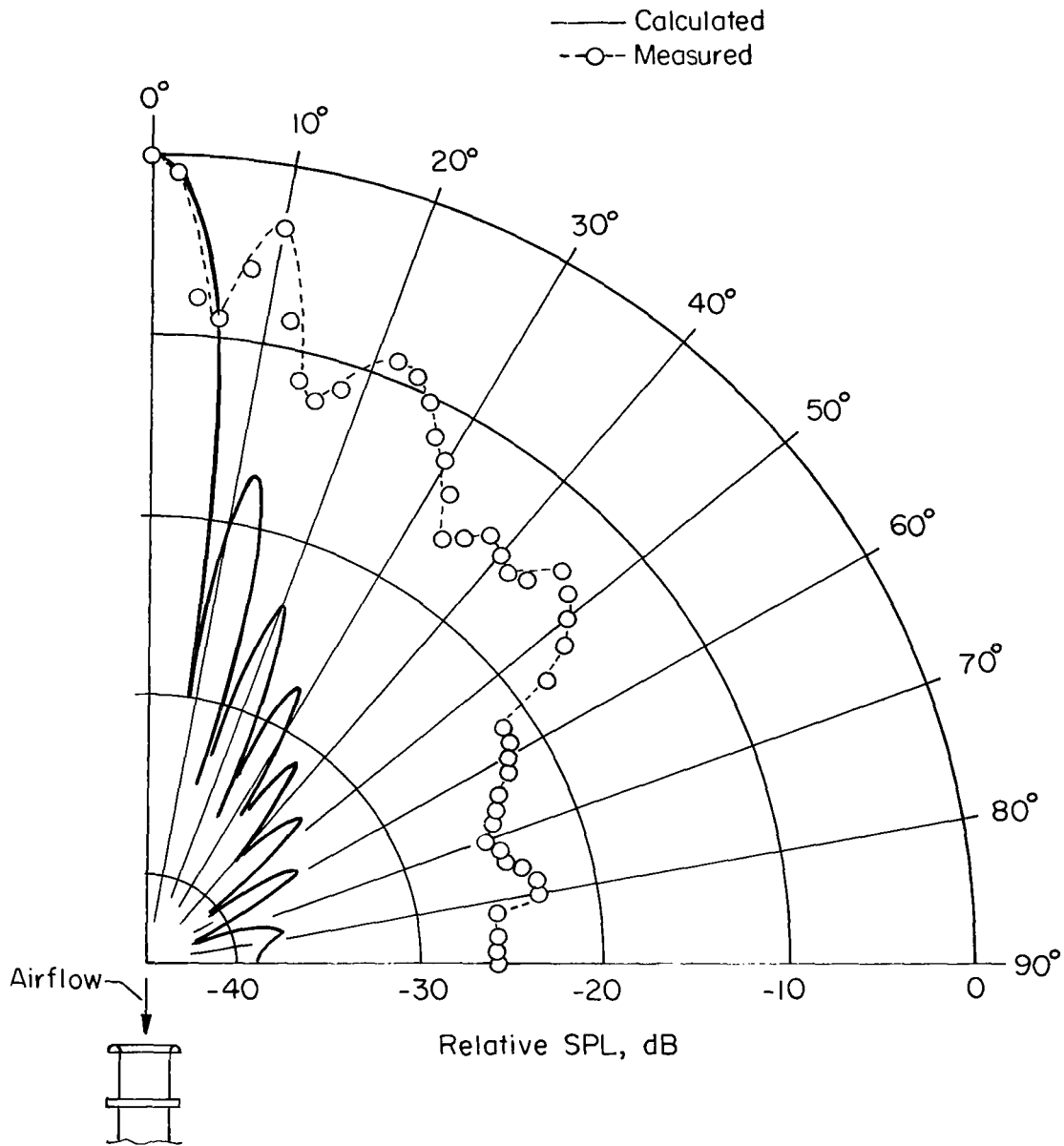
(d) Rotor with 53 guide vanes.

Figure 10.- Concluded.



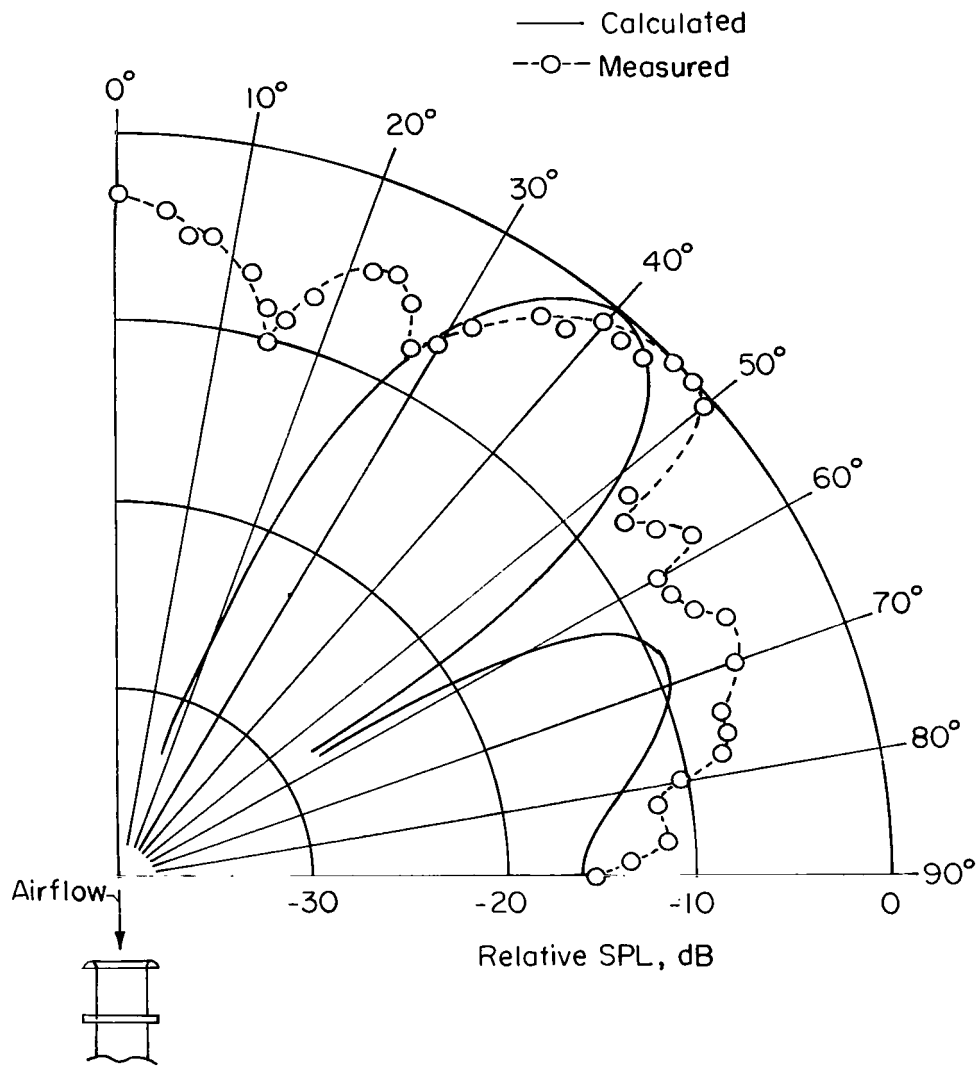
(a)  $M_t = 0.219$ ;  $\epsilon_m = 3.03$ .

Figure 11.- Calculated and measured one-third octave (at blade passage frequency) radiation patterns for the rotor-53-guide-vane configuration at two rotor tip speeds.



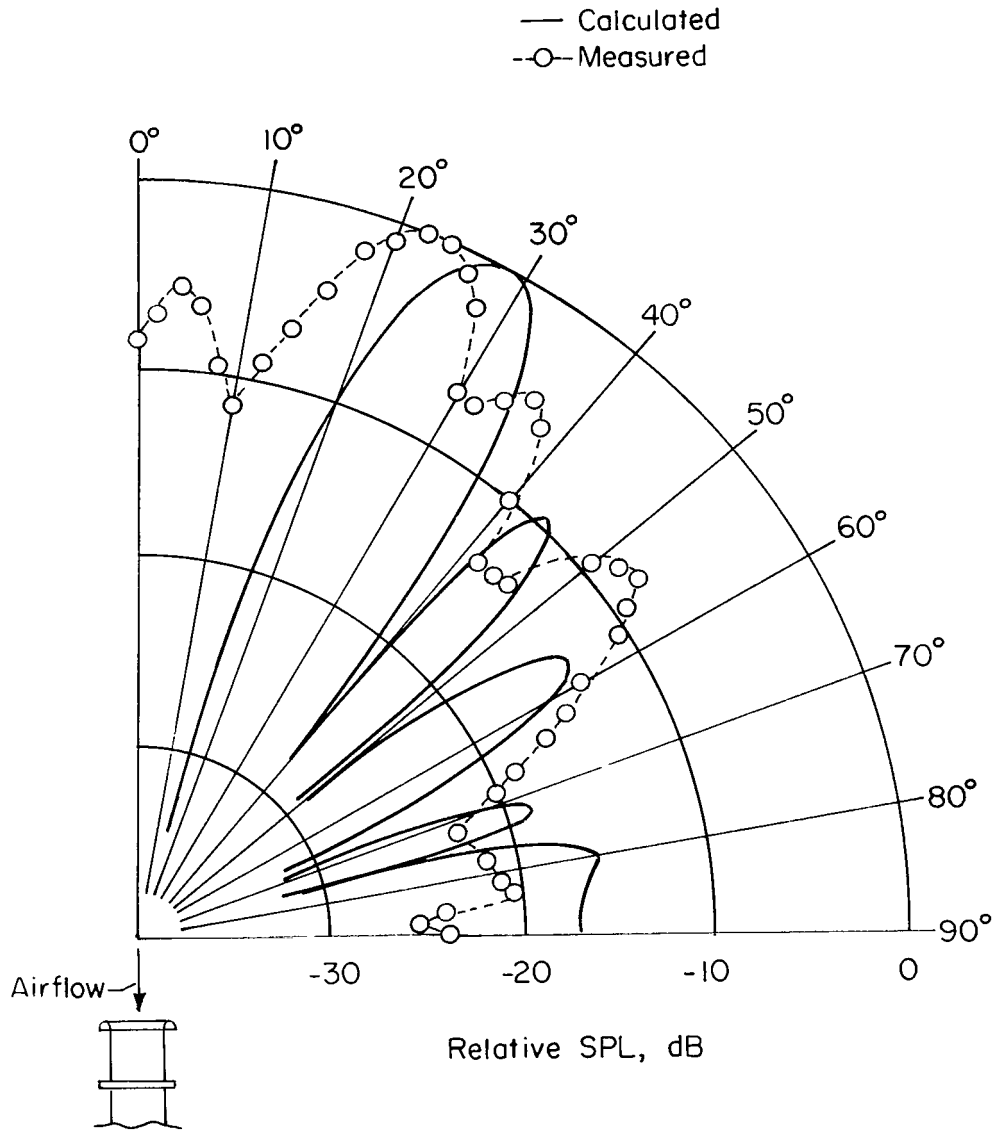
(b)  $M_t = 0.471$ ;  $\epsilon_m = 6.52$ .

Figure 11.- Concluded.



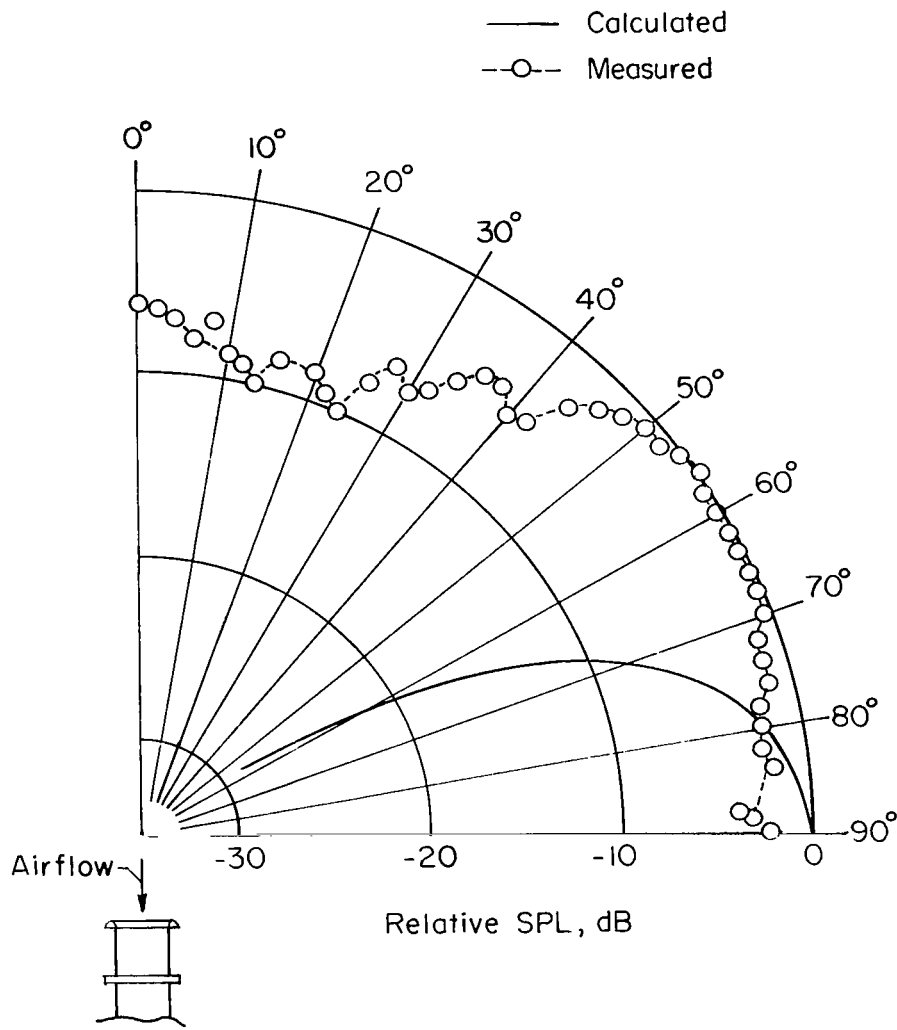
(a)  $M_t = 0.346$ ;  $\epsilon_m = 1.71$ .

Figure 12.- Calculated and measured one-third octave (at blade passage frequency) radiation patterns for the rotor—62-guide-vane configuration at two rotor tip speeds.



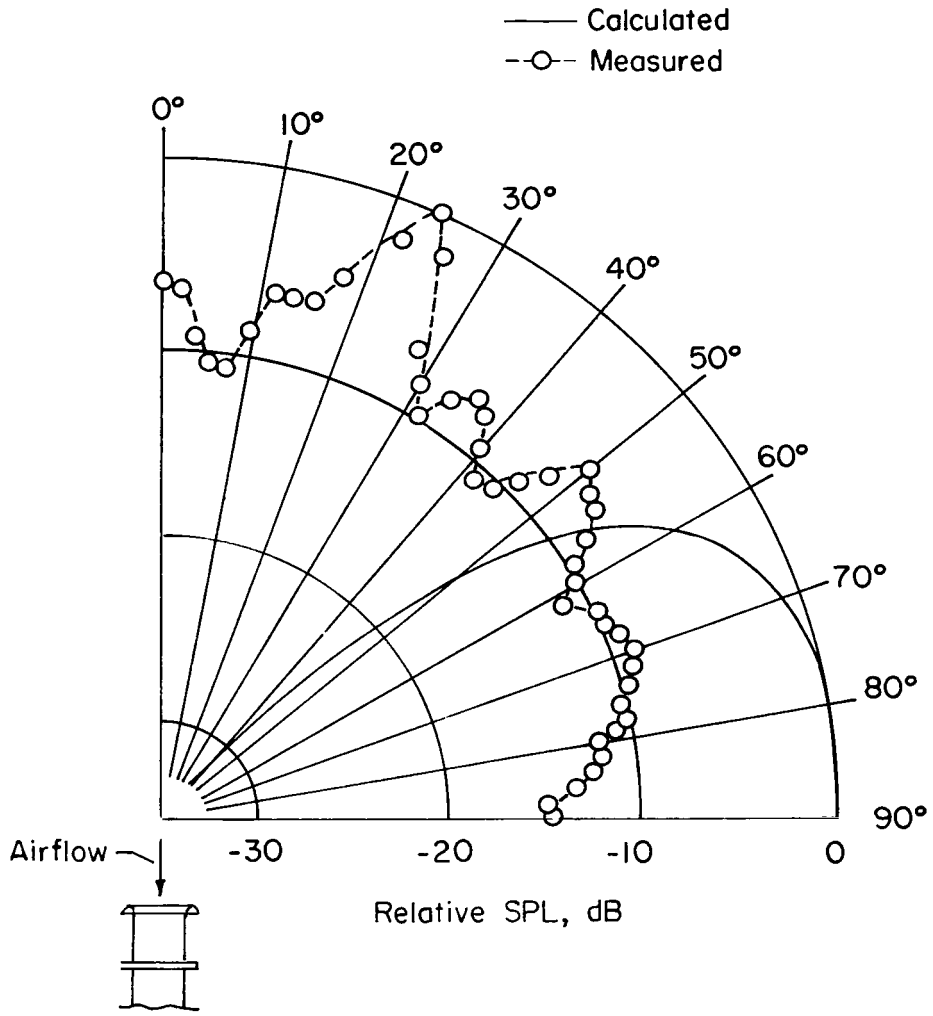
(b)  $M_t = 0.477$ ;  $\epsilon_m = 2.36$ .

Figure 12.- Concluded.



(a)  $M_t = 0.346$ ;  $\xi_m = 0.754$ .

Figure 13.- Calculated and measured one-third octave (at blade passage frequency) radiation patterns for the rotor-31-guide-vane configuration at two rotor tip speeds.



(b)  $M_t = 0.498$ ;  $\xi_m = 1.086$ .

Figure 13.- Concluded.

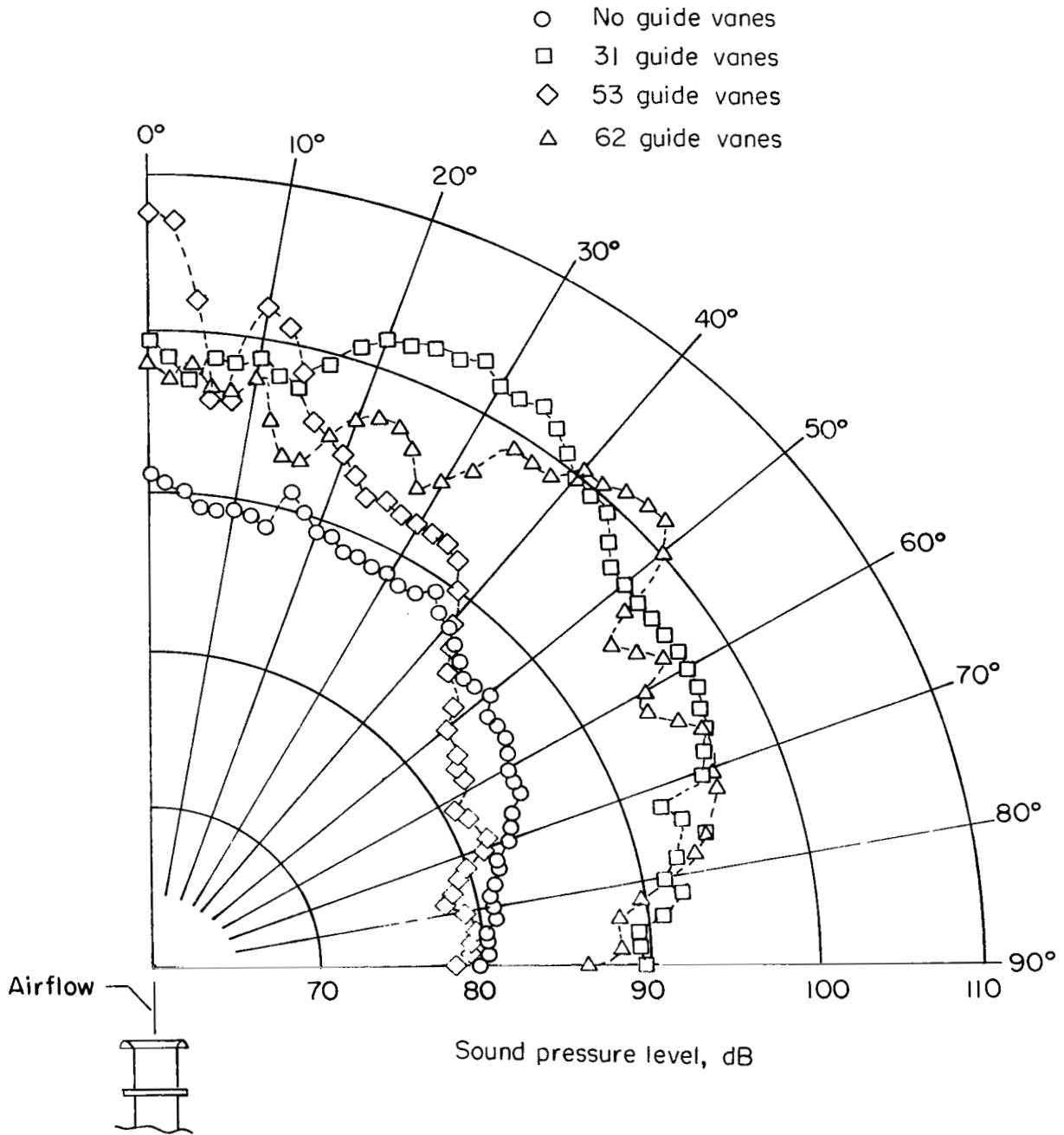
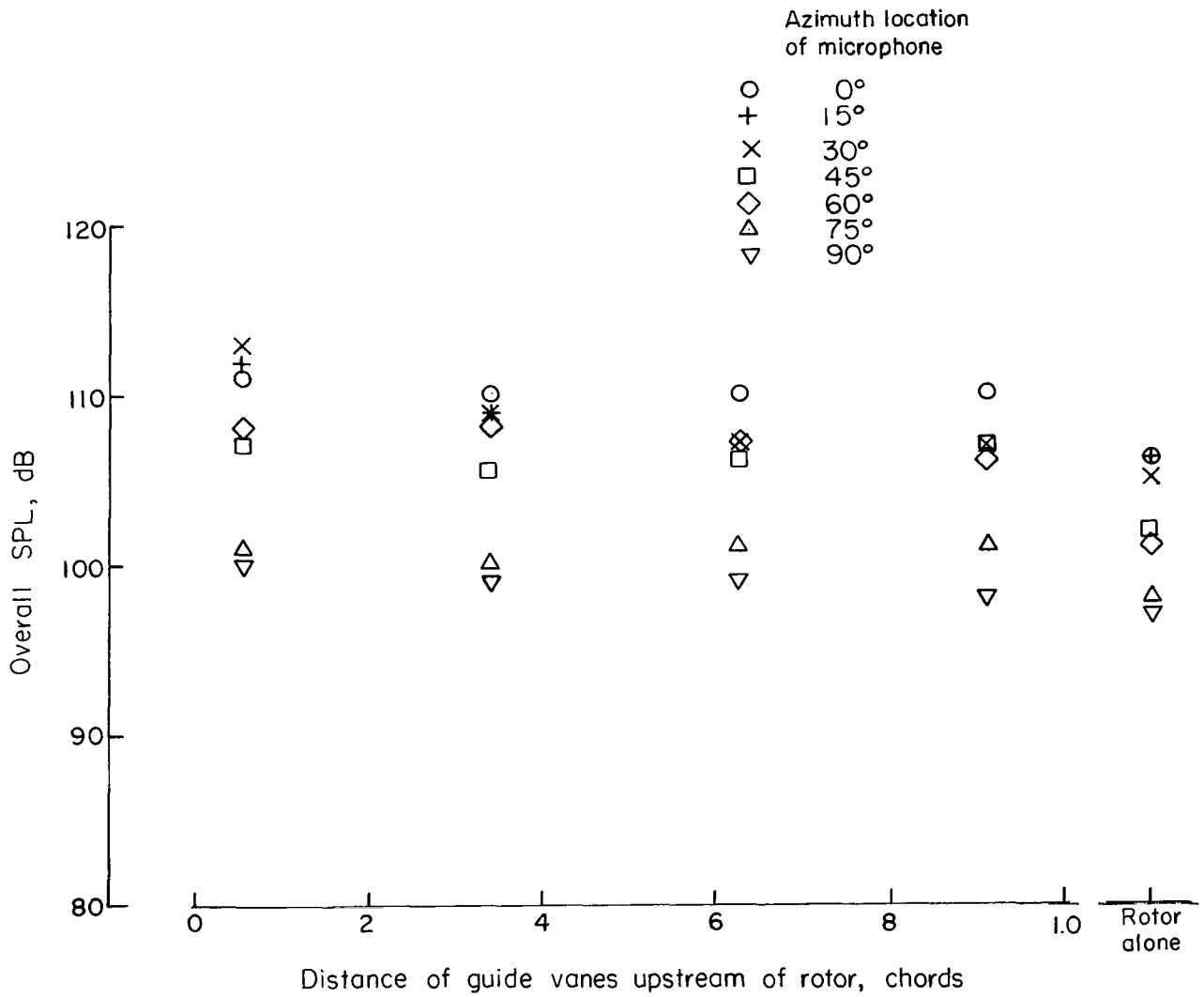
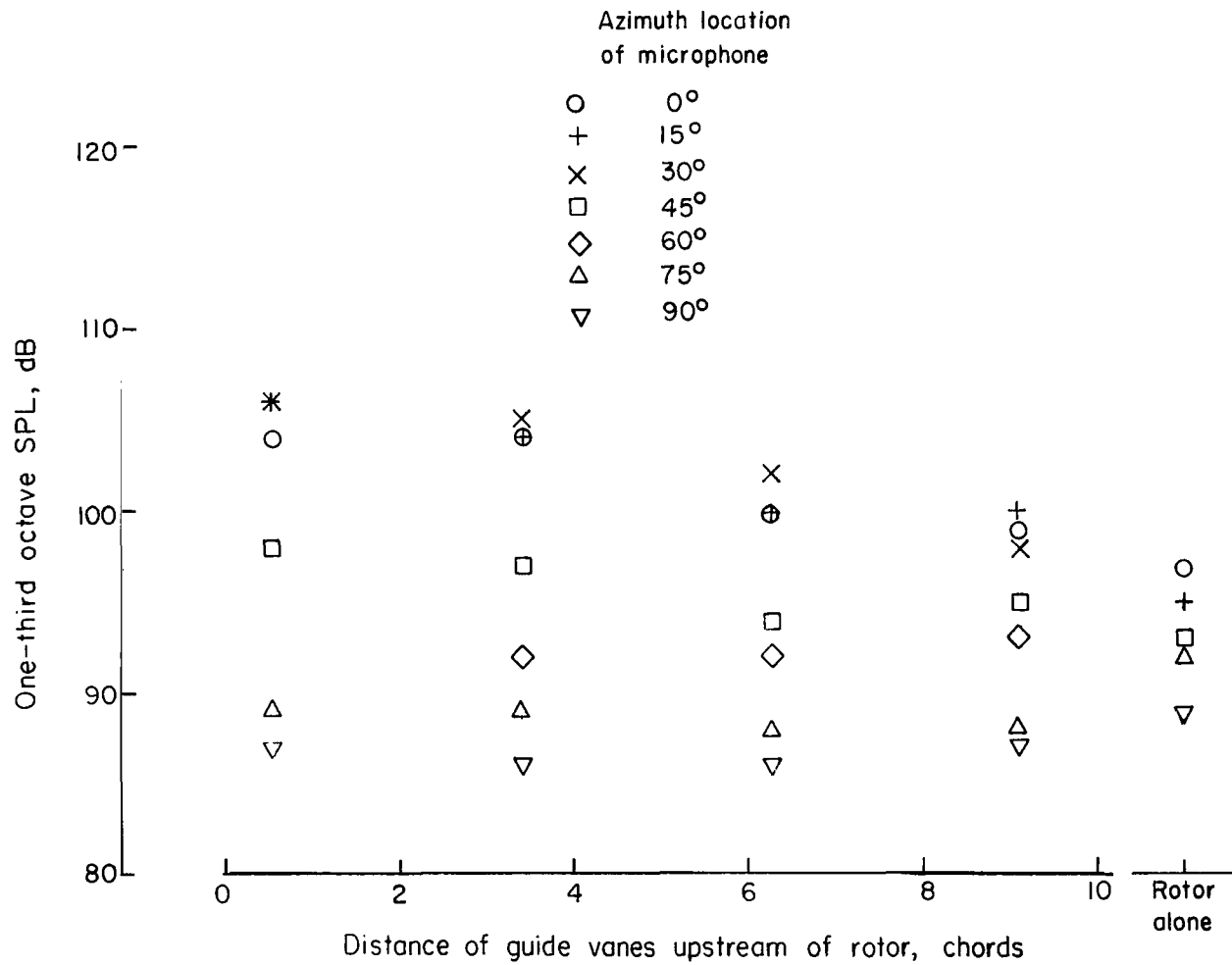


Figure 14.- Measured one-third octave (at blade passage frequency) radiation patterns for various rotor-guide-vane configurations.  $M_t = 0.346$ .



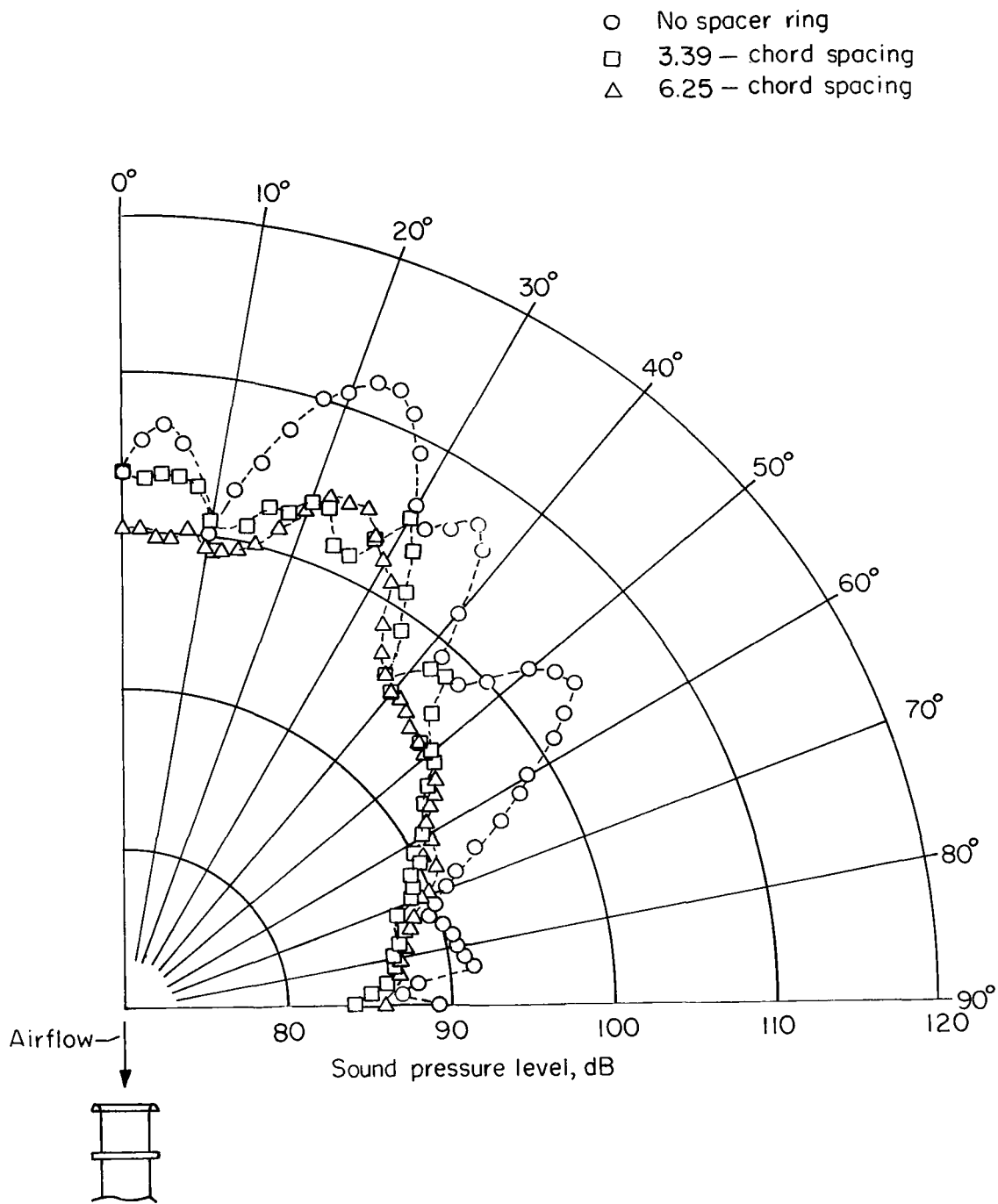
(a) Overall noise.

Figure 15.- Effect of rotor—guide-vane spacing on generated noise for 62-guide-vane assembly.  $M_t = 0.476$ ;  $\xi_m = 2.36$ .



(b) One-third octave filtered noise (centered at blade passage frequency).

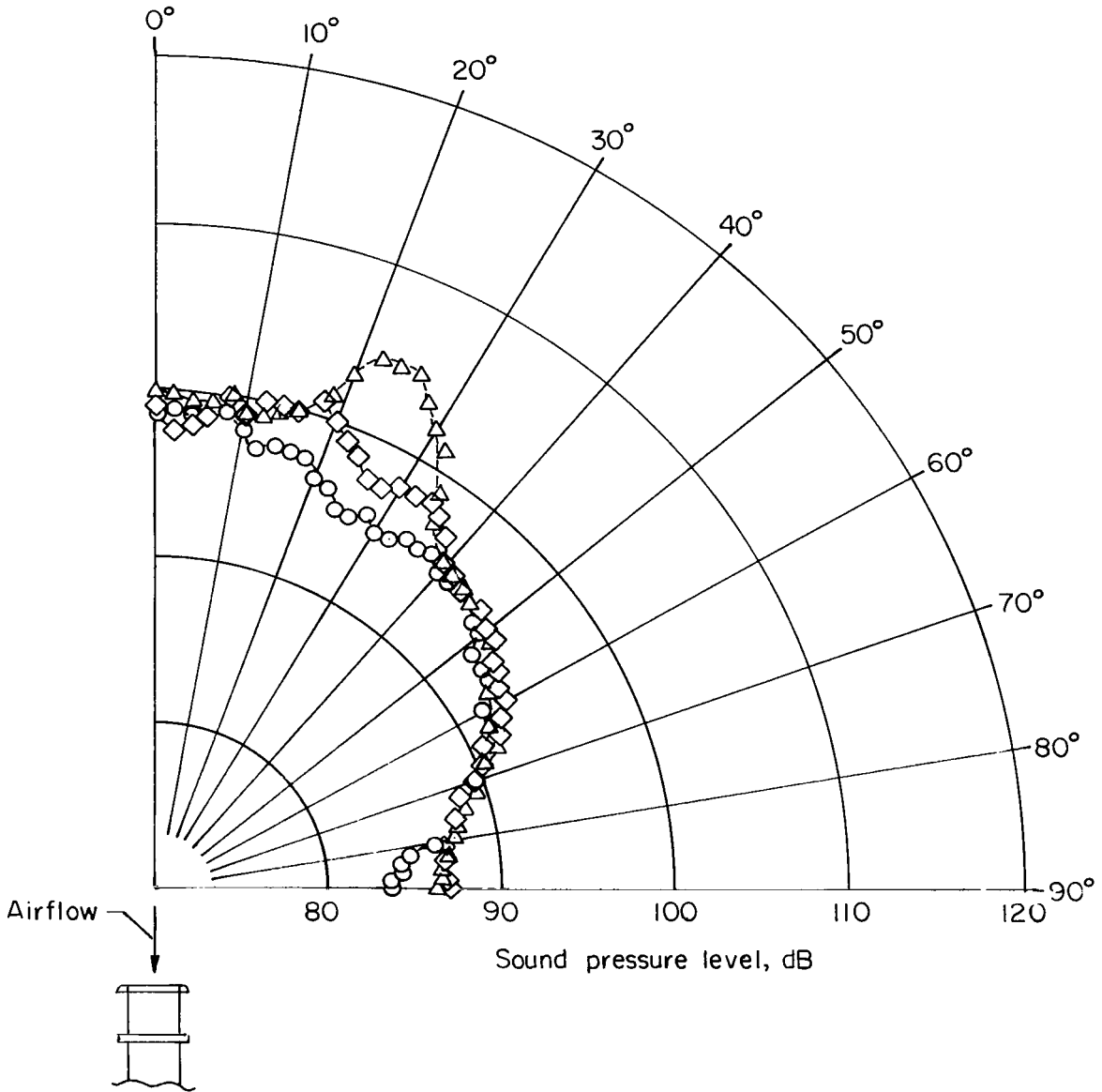
Figure 15.- Concluded.



(a) Radiation patterns for no spacer ring and for 3.39- and 6.25-chord spacings.

Figure 16.- Effect of rotor-inlet-guide-vane spacing on one-third octave (at blade passage frequency) radiation patterns for the rotor-62-guide-vane configuration.  $M_t = 0.477$ .

- △ 6.25-chord spacing
- ◇ 9.11-chord spacing
- Rotor alone



(b) Radiation patterns for 6.25- and 9.11-chord spacings.

Figure 16.- Concluded.

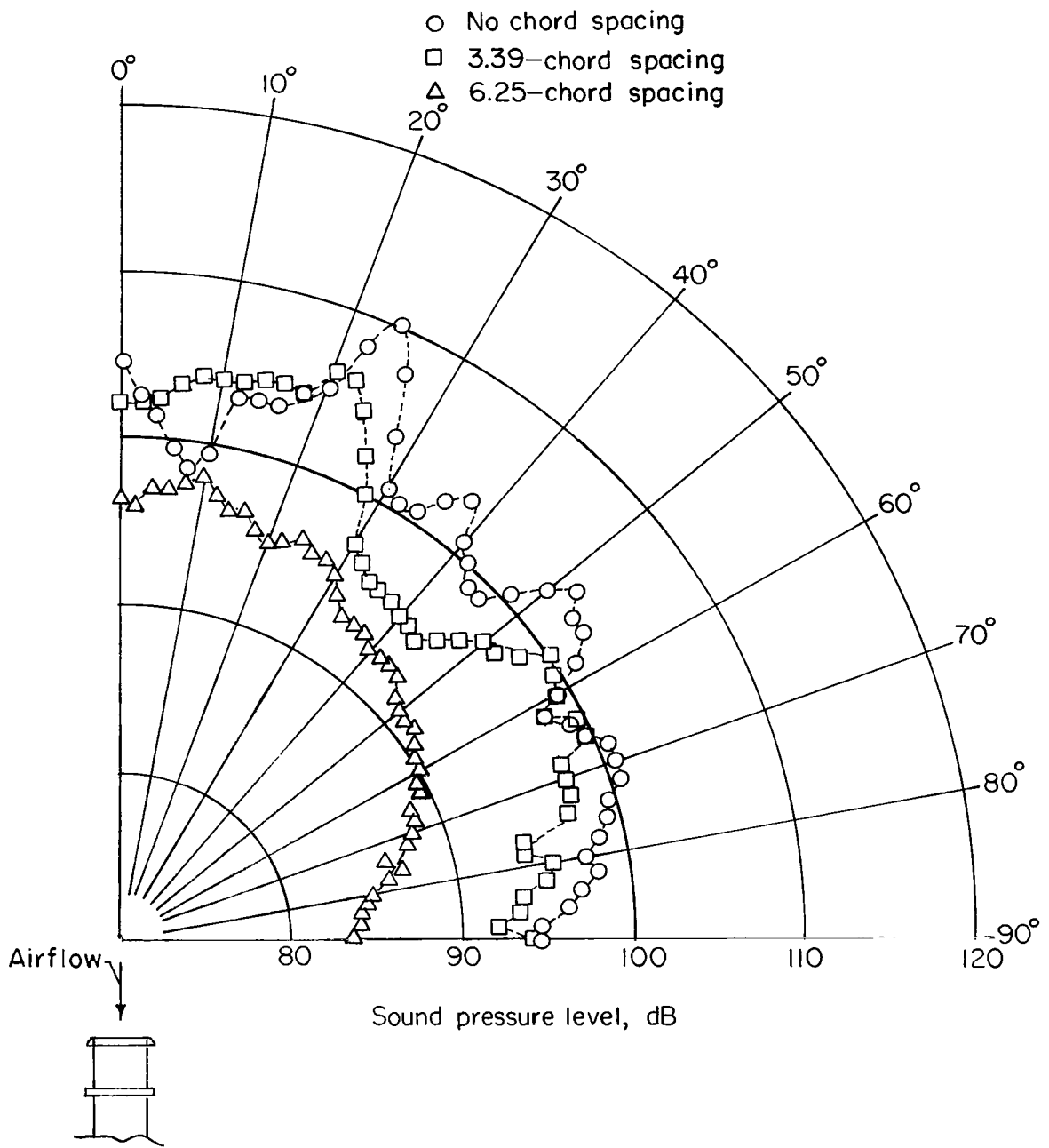


Figure 17.- Effect of rotor-guide-vane spacing on one-third octave (at blade passage frequency) radiation patterns for the rotor-31-guide-vane configuration.  $M_t = 0.498$ .

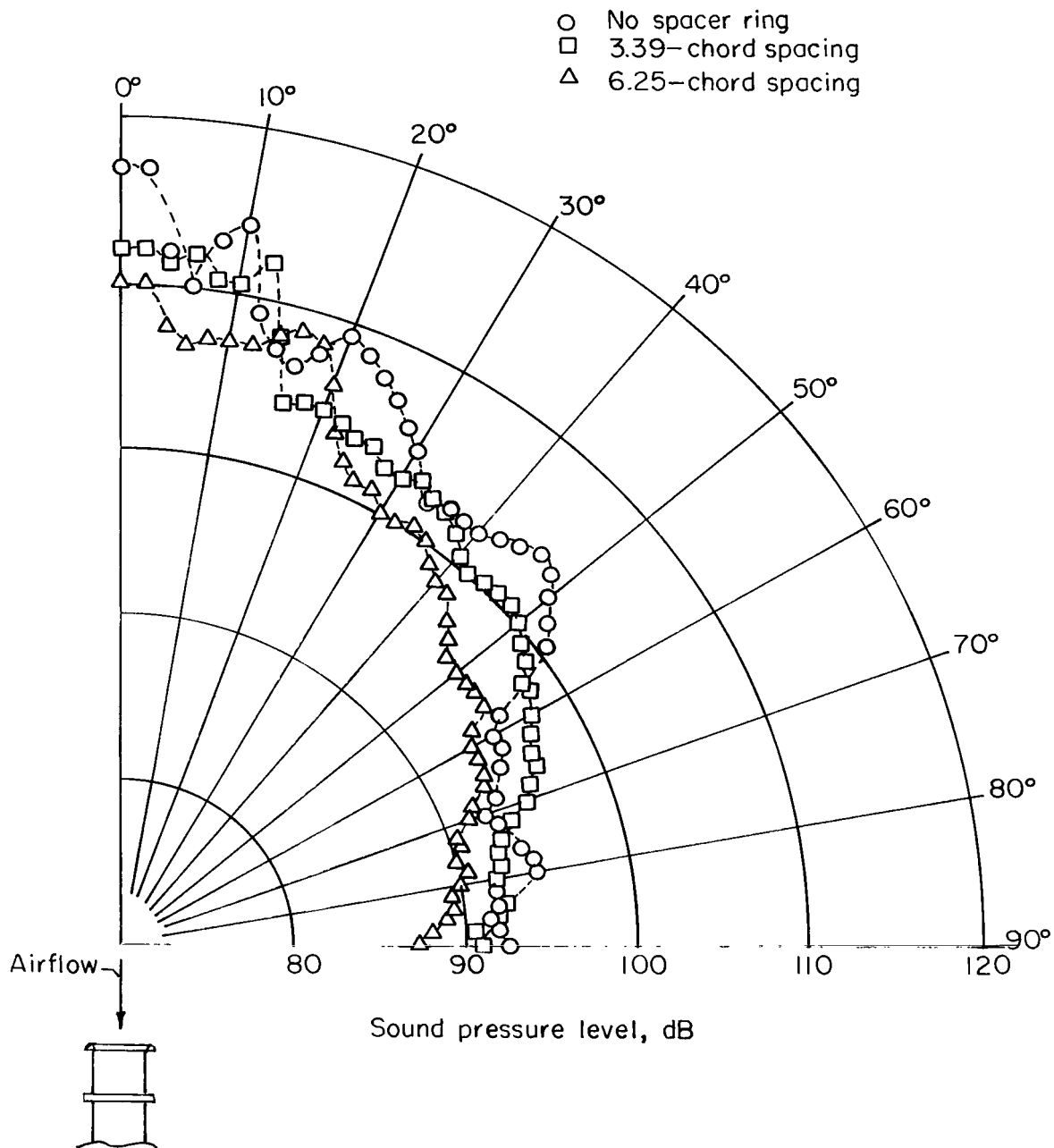


Figure 18.- Effect of rotor-inlet-guide-vane spacing on one-third octave (at blade passage frequency) radiation patterns for the rotor-53-guide-vane configuration.  $M_t = 0.471$ .

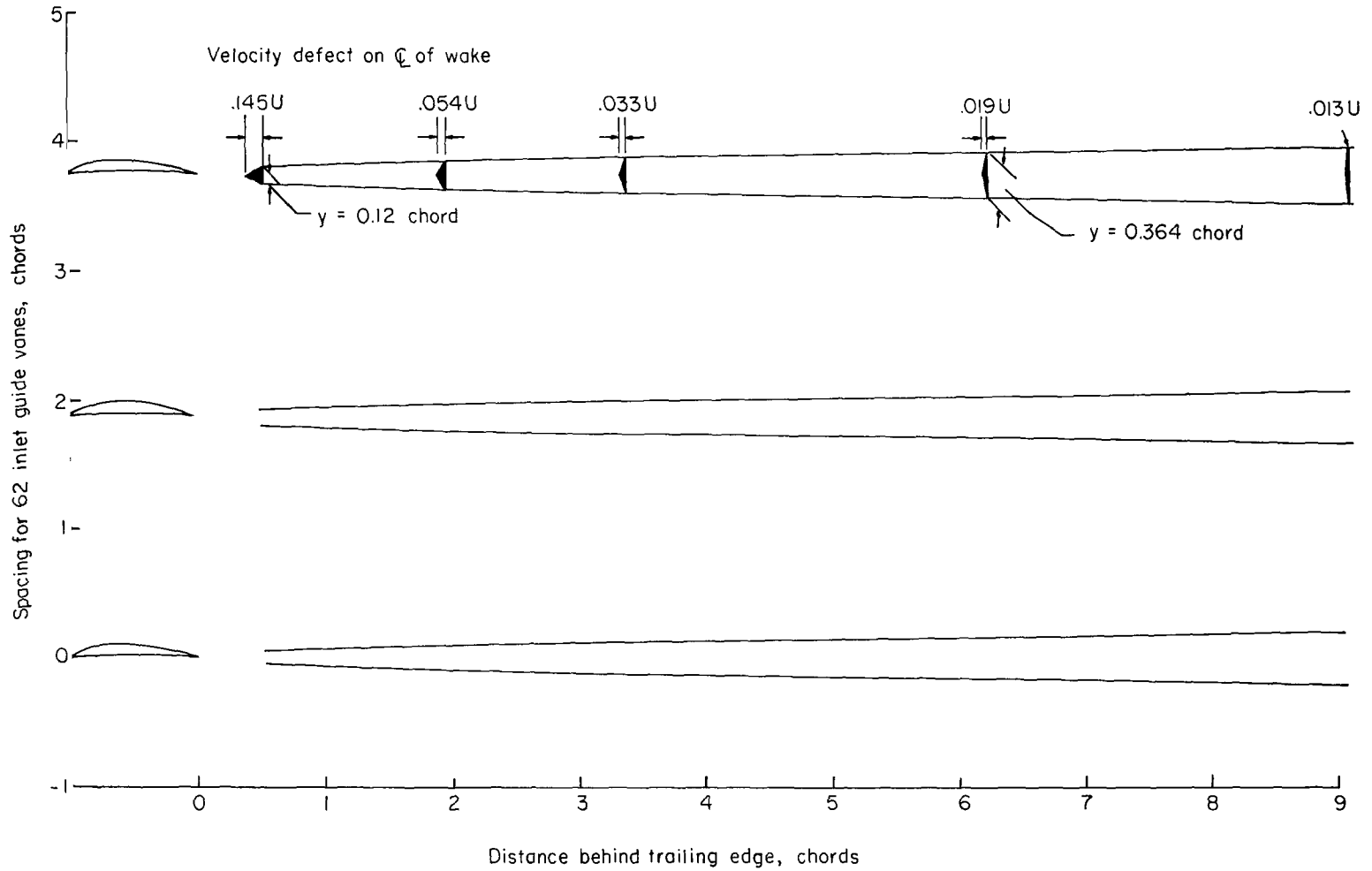


Figure 19.- Wake profile of guide vanes.  $C_{d,0} = 0.01$ .

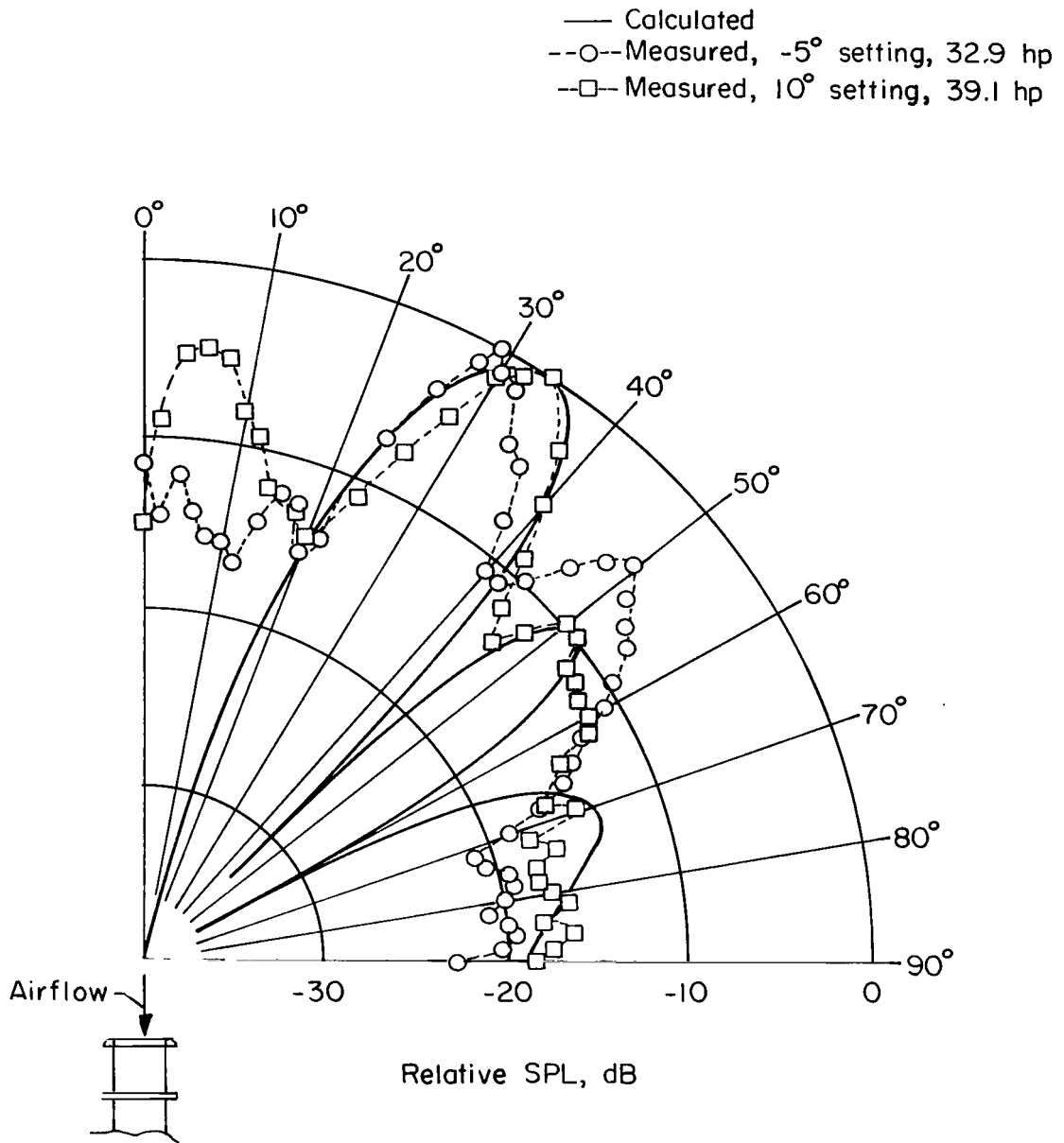


Figure 20.- Calculated and measured one-third octave (at blade passage frequency) radiation patterns due to stage loading and for rotor-62-guide-vane configuration.  $M_t = 0.418$ ; no spacer ring.

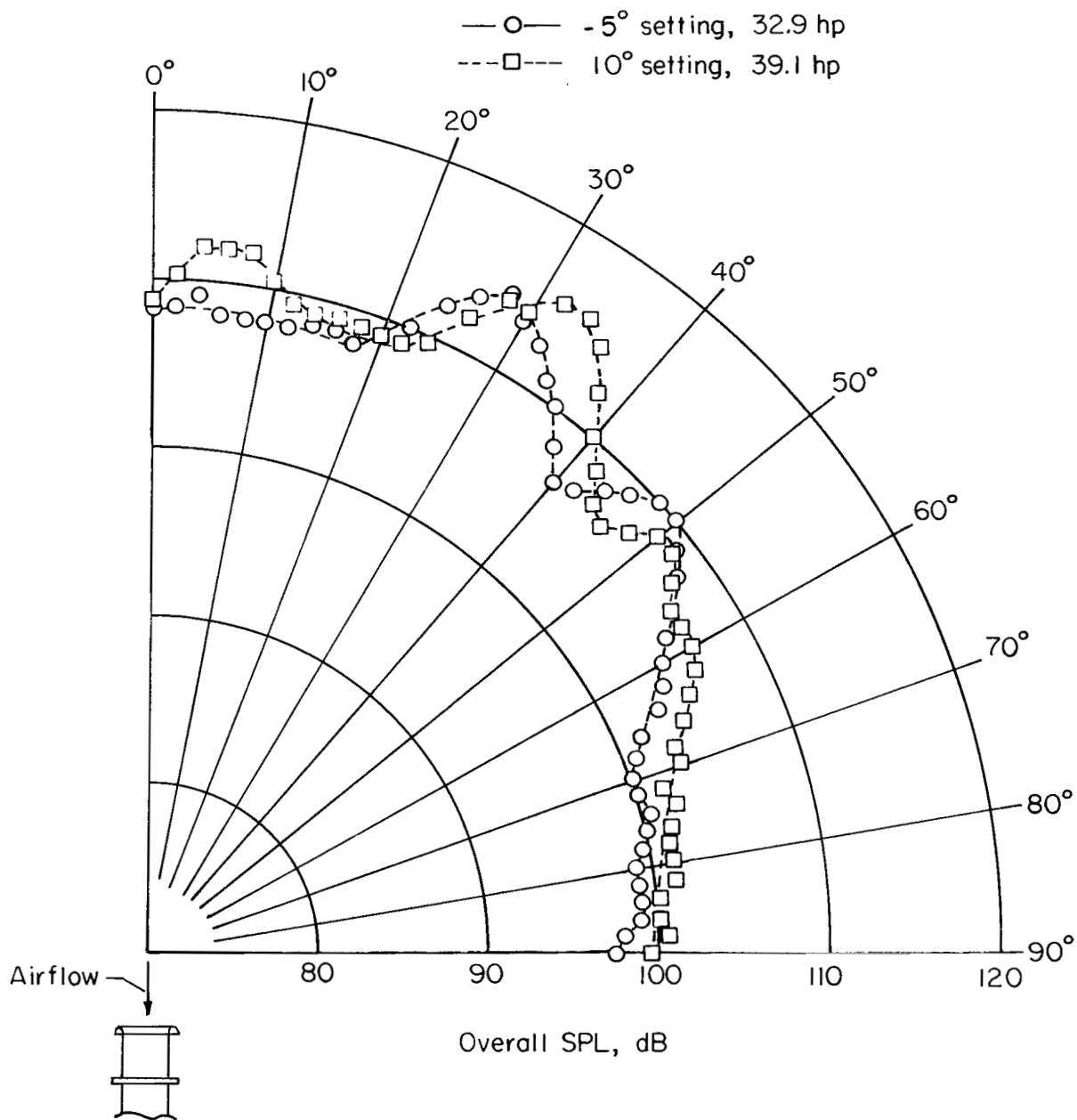


Figure 21.- Effect of stage loading on the measured overall noise radiation patterns for the rotor-62-inlet-guide-vane configuration.  $M_t = 0.418$ ; no spacer ring.

3/15/25

*"The aeronautical and space activities of the United States shall be conducted so as to contribute . . . to the expansion of human knowledge of phenomena in the atmosphere and space. The Administration shall provide for the widest practicable and appropriate dissemination of information concerning its activities and the results thereof."*

—NATIONAL AERONAUTICS AND SPACE ACT OF 1958

## NASA SCIENTIFIC AND TECHNICAL PUBLICATIONS

**TECHNICAL REPORTS:** Scientific and technical information considered important, complete, and a lasting contribution to existing knowledge.

**TECHNICAL NOTES:** Information less broad in scope but nevertheless of importance as a contribution to existing knowledge.

**TECHNICAL MEMORANDUMS:** Information receiving limited distribution because of preliminary data, security classification, or other reasons.

**CONTRACTOR REPORTS:** Technical information generated in connection with a NASA contract or grant and released under NASA auspices.

**TECHNICAL TRANSLATIONS:** Information published in a foreign language considered to merit NASA distribution in English.

**TECHNICAL REPRINTS:** Information derived from NASA activities and initially published in the form of journal articles.

**SPECIAL PUBLICATIONS:** Information derived from or of value to NASA activities but not necessarily reporting the results of individual NASA-programmed scientific efforts. Publications include conference proceedings, monographs, data compilations, handbooks, sourcebooks, and special bibliographies.

*Details on the availability of these publications may be obtained from:*

SCIENTIFIC AND TECHNICAL INFORMATION DIVISION  
NATIONAL AERONAUTICS AND SPACE ADMINISTRATION

Washington, D.C. 20546